Small Structures

small structures

www.small-structures.com

REVIEW OPEN ACCESS

Advancing Energy Storage Technologies Beyond Lithium With Cellulose-Derived Sustainable Carbon Materials

Vimukthi Dananjaya[1] | Nethmi Hansika[2] | Venkata Chevali[3] | Pratheep Kumar Annamalai[3] | Nisa Salim[1] | Lei Ge[3] | John Bell[3] | Satyanarayanan Seshadri[4] | Kothandaraman Ramanujam[4] | Ashok Kumar Nanjundan[3]

[1]School of Engineering, Swinburne University of Technology, Hawthorn, Australia | [2]Faculty of Engineering, Open University, Nawala, Sri Lanka | [3]Centre for Future Materials, School of Engineering, University of Southern Queensland, Springfield, Australia | [4]Department of Chemistry & The Energy Consortium, Indian Institute of Technology Madras, Chennai, India

Correspondence: Venkata Chevali (Venkata.chevali@unisq.edu.au) | Pratheep Kumar Annamalai (pratheep.annamalai@unisq.edu.au) | Ashok Kumar Nanjundan (Ashok.Nanjundan@unisq.edu.au)

Received: 16 August 2025 | **Revised:** 5 October 2025 | **Accepted:** 9 October 2025

Keywords: batteries | cellulose carbonization | hybrid systems | postlithium energy storage | supercapacitors | sustainable carbon

ABSTRACT

The transition to sustainable, high-performance alternatives to lithium-ion systems is accelerating research progress in electrochemical energy storage. Cellulose-derived carbons, made from abundant, renewable biomass, are emerging as promising candidates, offering natural environmental friendliness, adjustable structure, and functional versatility. This review examines the hierarchical architecture of cellulose, its carbonization pathways, and the influence of extraction and processing methods on precursor properties. Advances in synthetic techniques, from heteroatom doping to creating composite hybrids, are discussed for their role in controlling porosity, conductivity, and electrochemical behavior. Structure-property relationships and function of these carbons are analyzed in the context of sodium-, potassium-, zinc-, and magnesium-ion batteries, as well as hybrid supercapacitors. Important material properties, including electrical conductivity, mechanical strength, thermal stability, and morphological control, are analyzed in relation to device performance. Challenges related to scalability, electrolyte compatibility, and cycle life are addressed, with a focus on sustainable synthesis and integration routes. This review uniquely integrates cellulose-derived carbon across multiple postlithium energy storage systems with a focus on scalable synthesis and electrochemical optimization.

1 | Introduction

Globally, the demand for efficient and sustainable energy storage solutions is growing due to the increasing adoption of renewable energy and the electrification of transportation [1]. pies (LIBs) have been a leading energy storage technology for many years, and are now being used to power consumer electronics, electric vehicles, and grid storage systems [2, 3]. The global lithium reserve is estimated at 22 million tons, while sodium and potassium are 1,000 times more abundant, providing a more sustainable option for large-scale energy storage. The long-term prospects of LIBs are threatened by limited lithium resources, increasing material costs, and safety concerns, including dendrite growth and thermal runaway [4]. These problems have spurred the search for alternative energy storage methods that utilize more abundant and less expensive materials [5]. Besides lithium (postlithium), energy storage technologies like sodium-ion (SIBs), potassium-ion (KIBs), zinc-ion batteries (ZIBs), as well as magnesium-ion (MIBs), calcium-ion (CIBs), zinc-ion (ZIBs), aluminum-ion (AIBs), lithium–sulfur (Li–S), and lithium–air ($Li–O_2$) batteries (Figure 1) have gained significant interest [7]. These new technologies need electrodes with high capacity,

Vimukthi Dananjaya and Nethmi Hansika contributed equally to this study.

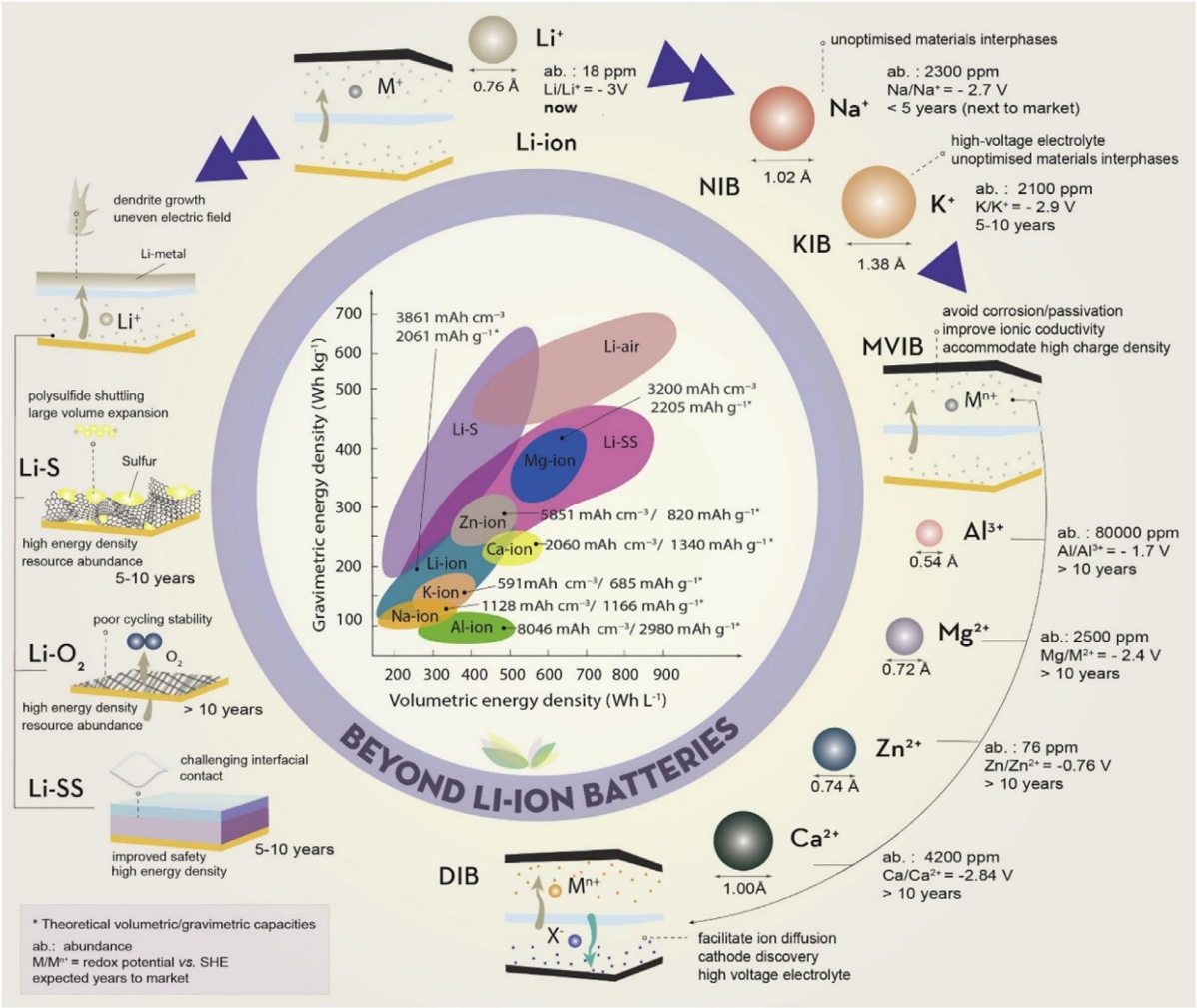

FIGURE 1 | Current state and challenges of LIBs. Graph depicting beyond LIBs: (left) anodes based on Li-metals (Li–S, Li–O_2, Li–SS) and (right) anodes based on Na, K, Al, Mg, Zn, and Ca, along with their global abundance and standard redox potential. It outlines their main advantages and challenges, as well as the volumetric and gravimetric energy densities and theoretical capacities that are currently achievable. Copyright 2022, Cell Press [6].

fast charging and discharging capabilities, and extended cycle life [1–3, 7, 8].

Advancements in sustainable and cleaner materials for post-LIBs are afforded by the development of renewable and abundant components that offer superior electrochemical performance. SIBs and KIBs stand out because of their chemical similarity to LIBs and the natural abundance of their respective charge carriers. However, the successful commercialization of these technologies depends on developing high-performance electrode materials that can accommodate larger ion sizes, provide fast charge and discharge capabilities, and sustained stability [9]. Carbon-based materials are considered indispensable for next-generation energy storage due to their high electrical conductivity, adjustable microstructure, and chemical stability [10]. While graphite has been traditionally used as an anode material in LIBs, it is not suitable for sodium and potassium storage because the larger ionic radii of Na^+ and K^+ make intercalation difficult. As a result, alternative disordered carbon materials, including hard carbon, porous carbon, and heteroatom-doped carbon, were explored for post-LIBs applications [11]. Among the various precursors used to create these materials, biomass-derived carbon has gained particular popularity due to its sustainability, affordability, and capacity for customization through structural engineering [12–15].

Much attention has been given to cellulose-derived carbon due to its renewable nature, abundance, and excellent carbonization potential [15]. Cellulose, an organic polymer derived from plant-based raw materials, serves as a green precursor for sustainable carbon. For energy storage applications, these carbon structures are highly valuable because of their high surface area, adjustable porosity, and good conductivity. As we move toward greener and cleaner energy systems, cellulose-derived carbon is now a viable alternative to conventional lithium for next-generation energy storage devices [16–18]. The flexible structure of cellulose-derived carbon makes it an ideal candidate due to its tunability. Adjusting morphology and structure through a carbonization process enhances ion transport, conductivity, and electrochemical stability, thereby improving overall performance [19, 20]. Besides batteries, cellulose-derived carbon also attracts research interest for supercapacitors and hybrid energy storage systems, particularly from the perspective of energy and power density [21]. The inherent properties of cellulose-like

hierarchical structures and porosity can be utilized in designing carbon materials to support rapid ion diffusion and high charge storage capacity [22]. Furthermore, various forms of functionalization of cellulose-derived carbon with elements and compounds enable the tailoring of electrochemical properties to further enhance energy storage performance. This adaptability makes cellulose-derived carbon highly promising for addressing energy storage challenges beyond those of lithium-based systems [21, 22].

Carbon from cellulose has many advantages, but its application in energy storage and large-scale production faces several challenges [23]. While optimizing synthesis methodologies is essential for ensuring consistent and reproducible properties, another key concern is scaling up production processes. Additionally, most postlithium battery chemistries require further research into the compatibility of cellulose-derived carbon with electrolytes and its long-term stability [24]. A complete realization of the potential of cellulose-derived carbon for future energy storage applications requires solving these critical issues. The growing body of research shows significant progress in cellulose-derived carbon, especially for postlithium energy storage, highlighting its potential and ongoing challenges [25]. Recent publications have focused on improving synthesis techniques, optimizing carbonization parameters, and exploring electrochemical compatibility with various electrolyte systems [14, 26]. Moreover, contemporary research investigations stress the urgent need for scalable, environmentally friendly manufacturing processes and enhanced stability under operational conditions. This review consolidates these findings by identifying key knowledge gaps and providing a framework for advancing cellulose-derived carbon materials. It also aims to guide future research toward sustainable, high-performance energy storage technologies, ensuring that innovations are scientifically sound and practical for industry [23, 24].

In this review, we explore recent progress in cellulose-derived carbon materials for energy storage technologies beyond lithium-ion systems. We focus on advances in synthesis strategies, structural tuning, and electrochemical performance, while also identifying critical gaps in the field, particularly the need to better understand how carbonization parameters influence electrochemical behavior. We emphasize the importance of developing green, scalable synthesis approaches. Looking ahead, we discuss the potential role these materials could play in future battery chemistries and hybrid storage systems and offer our perspective on the key challenges and opportunities that lie on the path toward high-performance, sustainable carbon-based energy storage solutions.

2 | Cellulose and Its Chemistry

Cellulose is the most abundant natural biopolymer, and a long-chain linear polymer (polysaccharide) made up of repeated D-glucose units connected through β−1, 4- glycosidic linkages [27]. Its unique molecular structure, defined by extensive intra- and intermolecular hydrogen bonding, creates both crystalline and amorphous regions within cellulose, leading to fiber formation. These structural features provide mechanical strength and thermal stability while also affecting its solubility, reactivity, and potential as a precursor for functional carbon materials [28]. A variety of functional properties can be added to cellulose by chemically modifying its hydroxyl groups. This flexibility makes -OH functionality a key design aspect for developing cellulose-based materials.

2.1 | Structure, Properties, and Carbonization of Cellulose

Due to the hierarchical structure of cellulose, different polymorphs are formed, depending on the chain orientation and hydrogen bonding patterns (Figure 2) [29–31]. Cellulose I (native or blue cellulose), cellulose II (mercerized/regenerated cellulose), cellulose III (cellulose II dissolved in ammonium sulfite), and cellulose IV (formed when cellulose II is heated) are the other allomorphs of cellulose [32, 33]. These polymorphs exhibit distinct thermal and chemical behaviors, which directly impact their carbonization efficiency and properties of the resultant carbon [33]. The crystalline regions enhance thermal resistance, while the amorphous regions provide sites for chemical modification and contribute to the evolution of porosity during carbonization.

The hydrogen bonding network in cellulose provides resistance to chemical and thermal degradation. In extreme conditions, such as very high temperatures or highly acidic or basic environments, the chemical structure of cellulose causes depolymerization, producing simpler sugar molecules [34]. Its thermal stability is noticeable between 200 and 400°C, depending on the degree of crystallinity and moisture content [35]. Water disrupts hydrogen bonds, leading to the breakdown of cellulose or promoting hydrolysis [34–36]. Cellulose contains “renewable carbon” that theoretically makes up 44 wt%, which can be converted into various forms of carbon, including amorphous, graphitic, and porous structures. This ability to transform makes cellulose a highly suitable precursor for energy storage applications [37]. To achieve this, the graphitization potential of cellulosic materials is enhanced through high-temperature carbonization (>1000°C) and subsequent catalytic activation, producing conductive carbon suitable for electrodes in postlithium batteries, such as sodium-ion, potassium-ion, and hybrid systems [37–39].

2.2 | Sources and Isolation of Cellulose

Cellulose is a pervasive component in the cell walls of plants, algae, and certain bacteria. Woody plants are the most common source of cellulose, containing ≈40%–50% by weight, making them an ideal source for industrial cellulose extraction [40]. Other significant cellulosic sources include cotton (over 90 wt%), hemp, flax, and agricultural waste such as straw. Additionally, bacterial cellulose (BC), obtained from bacteria such as *Gluconacetobacter xylinum*, which is present in plant cell polysaccharides, is considered a superior source; however, the isolation and purification of this material are commercially prohibitive.

Extraction methods vary depending on the source and the required purity. Cellulose is most commonly isolated by the Kraft process, in which sodium hydroxide and sodium sulfide are used to break down noncellulosic components of the pulp. In contrast, sulfite pulping employs acidic or neutral bisulfite

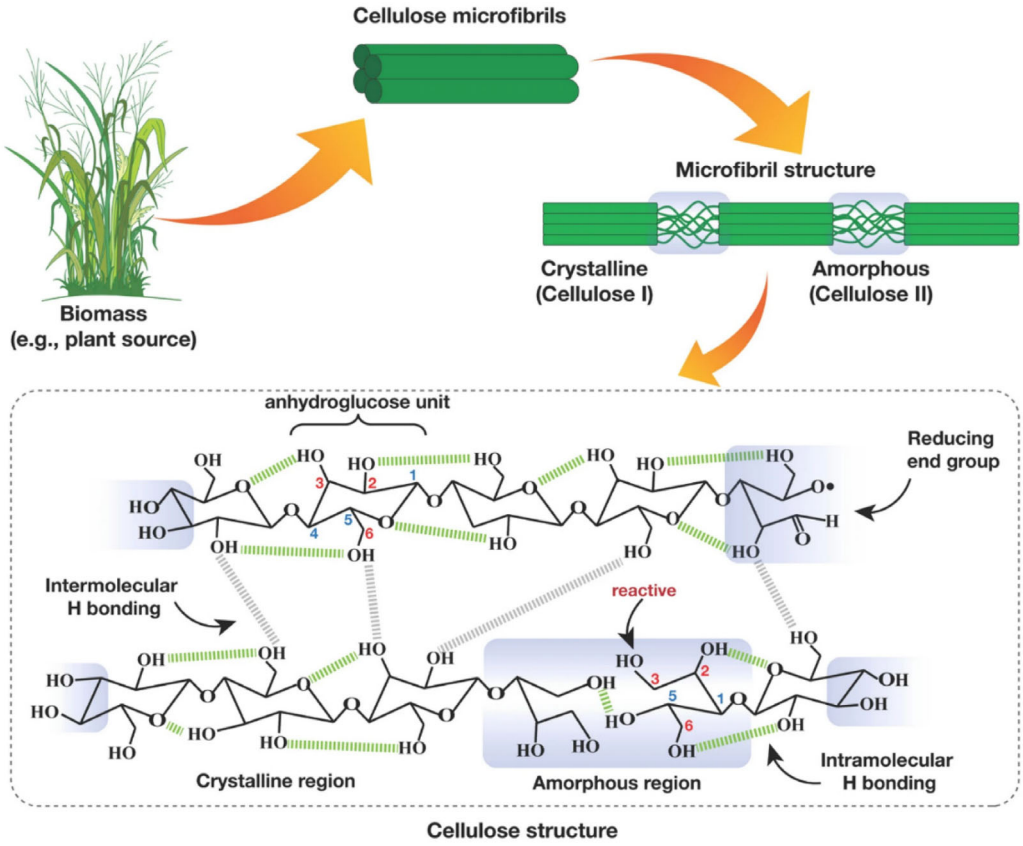

FIGURE 2 | Hierarchical structure of cellulose from plant biomass to molecular structure showing different functional groups and reactive sites embedded in crystalline (ordered) and amorphous (disordered) regions. Copyright 2022, Springer Nature [29].

solutions to delignify and bleach wood pulp [41]. Mechanical cellulose extraction involves physical means to break down plant biomass, often combined with minor chemical processes, to produce cellulose. These methods vary in their effectiveness in purifying cellulose, depending on the source of cellulose and the anticipated purity of the product [41]. Besides chemical and mechanical methods of cellulose extraction, processes such as organic pulping are effective because lignin is dissolved in organic solvents, like ethanol, rather than creating bulky waste. Enzymatic digestion of wood is another standard method to remove noncellulosic components. Chemical extraction techniques are currently preferred for cellulose extraction due to their effectiveness and cost efficiency; however, with advances in green chemistry, developing sustainable methods to improve cellulose extraction is becoming increasingly important [41, 42].

Cellulose offers a natural option for modifying carbon structures due to the diverse composition and morphology of its lignocellulosic source, as well as its underlying hierarchical structure and chemical diversity [43]. Specifically, the carbonization behavior of different plant parts varies depending on their lignin, cellulose, and hemicellulose content, which dictate the structural and electrochemical profile of the carbon produced [44]. Understanding these differences is crucial for creating carbon materials tailored for specific industrial uses, especially in energy storage, catalysis, and adsorption technologies.

Recently, studies on the influence of cell wall variations demonstrated the versatility of biomass by analyzing the carbonization behavior of different sections of sorghum, including leaf, sheath, and stem. As each section possesses a unique lignocellulosic composition and morphology, it results in varied carbon yields, porosities, crystallinities, and graphitic features [45]. For instance, a biomass part with higher lignin content tends to produce more graphitic carbon with a greater degree of ordering. Conversely, sections with higher cellulose content generate carbon with larger interlayer spacing and more disorder. Although biomass selection is often based on its natural composition and shape, our recent study showed that these parameters can be effectively altered with a one- or two-step biorefining process at minimal concentrations. By carefully modifying the lignocellulosic composition of sorghum, carbon with increased porosity and surface area was produced from cellulose-rich precursors, enhancing specific capacitance. For instance, a mild alkali treatment (2 w/v.% NaOH) selectively removed noncellulosic components from sorghum biomass, thereby controlling the carbonization behavior and improving these structural characteristics. Further bleaching treatment (with sodium hypochlorite/acetic acid system) enhanced the crystalline cellulose content in the precursor, resulting in a highly porous carbon [46]. These results demonstrate the ability to tune biomass-derived carbon through targeted chemical treatments, providing precise control over structure and electrochemical development [45, 46].

2.3 | Modification of Cellulose

Natural hierarchical porosity is a key advantage of cellulosic materials as carbon precursors [47]. The intrinsic micro- to macroporous structure of cellulose-derived carbon enables effective ion diffusion, which enhances charge storage and electrochemical kinetics [48]. These properties can be further improved through chemical functionalization, particularly by modifying the reactive hydroxyl (-OH) groups of the cellulose backbone, a process known as cellulose functionalization (Figure 3) [49]. This process enables the introduction of new properties such as hydrophobicity, ion exchange capacity, or increased reactivity [50, 51]. Cellulose derivatives with enhanced solubility, thermal stability, and mechanical properties can be created through well-established synthetic methods, including esterification, etherification, oxidation, and graft polymerization [47]. Another common research strategy involves heteroatom doping of cellulose, followed by the incorporation into composites.

In addition to chemical functionalization, cellulose can be converted into cellulose-based nanomaterials (CNMs), which are nanoscale forms of cellulose that serve as versatile precursors for advanced carbon materials due to their hierarchical structure, high carbon content, and tunable properties [29]. CNMs have a strength of 1.6–3 GPa [52], low weight [53], and a surface area of $91.9 \pm 2.1\ m^2/g$, making them ideal for applications in energy storage and composite design [54]. CNMs include cellulose nanocrystals (CNCs), nanofibers (CNFs), or nanofibrillated cellulose (NFCs) and/or irregular nanoparticles (CNPs), each offering distinct structural and functional characteristics. CNCs are rod-shaped, highly crystalline particles produced by acid hydrolysis, enzyme degradation, or oxidative degradation of cellulose. Their rigid structure and high aspect ratio enable the formation of graphitic and porous carbon materials upon pyrolysis [3]. CNFs, obtained through mechanical fibrillation, enzymatic pretreatment, or oxidation, consist of entangled fibrils with both crystalline and amorphous regions. CNPs are spherical or irregularly shaped particles derived from hydrothermal treatment, ultrasonication, or precipitation techniques on cellulose. Retaining their postcarbonization nanostructure makes CNMs-derived carbons suitablefor supercapacitors and SIBs. Furthermore, their surface chemistry allows heteroatom doping, further enhancing charge storage capabilities.

Overall, cellulose stands out among sustainable carbon precursors for its inherent structural order, chemical tunability, and adaptability to nanoscale design. Its selective functionalization enables precise control over carbon yield, surface chemistry, and microstructure during pyrolysis. Through deconstruction into nanocrystals or nanofibrils, cellulose provides a facile route to hierarchical carbon architectures with high surface area, interconnected porosity, and tunable graphitic domains. These combined chemical and structural advantages promote efficient ion transport and electrochemical activity, making cellulose-derived carbons highly competitive against other biomass or synthetic sources.

3 | Carbonization Methods

Various methods have been developed for synthesizing cellulose-derived carbon, with the majority focusing on carbonization processes that produce conductive and porous structures. Among these, pyrolysis is a common technique that involves the thermal decomposition of cellulose in an inert atmosphere. Earlier studies

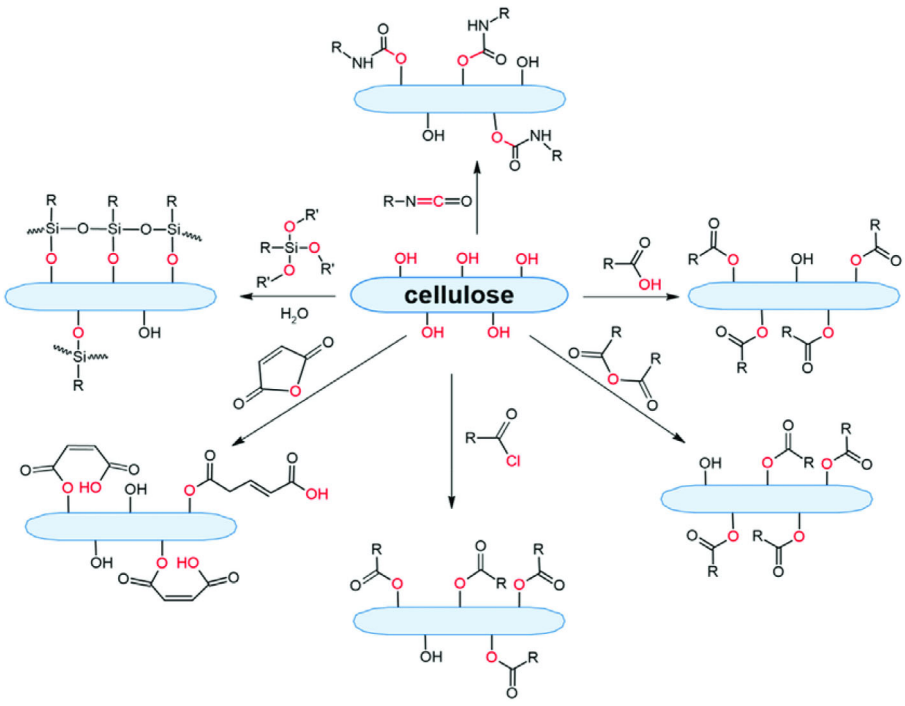

FIGURE 3 | Functionalization and modification of cellulose. Copyright 2022, MDPI [49].

have provided detailed insights into the reaction mechanisms behind this transformation, revealing a four-stage process during pyrolysis [55, 56]. The first stage involves the desorption of physically adsorbed water, which occurs at relatively low temperatures. As heating continues, the second stage focuses on removing structural water, primarily from -OH groups within the cellulose backbone. The third stage signifies a critical transformation, during which chain scission, depolymerization, and the breaking of C—O and C bonds occur. This stage is characterized by the release of volatile species, including water, carbon monoxide (CO), and carbon dioxide (CO_2), which leads to a gradual breakdown of the cellulose structure. Finally, the leftover carbon undergoes aromatization in the fourth stage, forming graphite-like layers [57].

Carbon atoms are considered to form graphitic domains when they are formed in cellulose ring units. These core studies offer a crucial framework for understanding how cellulose-derived carbon materials can be engineered by controlling pyrolysis conditions [58, 59]. The ability to manipulate these stages enables the design of carbon materials with specific porosity, graphitic content, and surface properties, making them valuable for applications in energy storage, catalysis, and structural purposes. Over recent decades, advancements in processing techniques and analytical tools have greatly improved our understanding and control over the transformation of cellulose into functional carbon materials [60]. Table 1 compares the processing techniques and conditions for cellulose carbonization and activation.

TABLE 1 | Processing techniques and conditions for cellulose carbonization and activation.

Method	Temperature range (°C)	Key features	Advantages	Disadvantages
Pyrolysis (for hard carbon)	700–1600	Microporosity, increased density	Small crystalline domains, well-established and easily scalable to an industrial level, produce high-quality carbons with controllable porosity and graphitization, wide precursor compatibility	High energy consumption, significant CO_2 and volatile emissions, requiring costly treatment, the environmental footprint is high compared to other methods.
Slow pyrolysis	400–800 (at <10°C min^{-1})	High porosity, preserved structure	Good structural integrity	Time-consuming
Fast pyrolysis	450–700 (at <100°C s^{-1})	Rapid heating, bio-oil byproducts	High throughput	Lower structural order, smaller particles
Chemical activation	400–900	KOH, H_3PO_4, $ZnCl_2$ used	High surface area, achieve very high surface area and tunable pore distribution, can tailor material for supercapacitors/batteries, moderate energy requirement compared to pyrolysis	Use of corrosive chemicals, hazardous to handle, large wastewater generation, raising environmental concerns, waste treatment, and chemical recycling challenges hinder large-scale adoption
Hydrothermal carbonization	180–280	Water-based, oxygen-rich surface	Low energy input, functional groups, water as a solvent makes it relatively eco-friendly, suitable for wet biomass without prior drying, retain oxygen functionalities useful for energy storage	Lower conductivity, needs post-treatment, generates wastewater that needs treatment, and the drying step increases cost
Microwave-assisted carbonization	300–800 (<10 min)	Rapid, energy-efficient	Fast, scalable, more uniform heating at a small scale, cleaner process with reduced emissions	Requires microwave absorbers, limited penetration depth restricts batch size, expensive equipment setup, industrial scalability not yet proven; better suited for lab/pilot scale
Electrochemical carbonization	23–200	Electric field-driven decomposition	Low temperature, tunable surface chemistry, very low energy demand, minimal emissions, and environmentally benign, enables precise functionalization and heteroatom doping during synthesis	Early stage, lower carbon yield, current scalability is poor compared to pyrolysis.

While the core carbonization process, including desorption of water, depolymerization, gas evolution, and aromatization, remains essential for creating cellulose-derived carbon materials, modern engineering methods have enhanced these steps beyond traditional pyrolysis to achieve specific properties such as porosity, conductivity, and structural integrity [44, 61]. Hydrothermal carbonization (HTC) is an example where water is used at high temperatures and pressure to convert cellulose into a carbon material [62, 63]. These methods involve activation techniques using different activating agents, such as potassium hydroxide (KOH), carbon dioxide (CO_2), or steam, to increase porosity and surface area. Additionally, there is template-assisted synthesis, which can be either hard or soft templating, to control the morphology of the produced carbon. Moreover, solvothermal and microwave-assisted methods are being explored for faster, more energy-efficient cellulose carbonization.

3.1 | Pyrolysis

Pyrolysis is the most common technique used in synthesizing cellulose-derived carbon, involving thermal decomposition in an oxygen-free or inert atmosphere such as nitrogen or argon. The typical temperatures range from 400 to 1000°C, depending on the desired carbon structure and properties [64]. Pyrolysis of cellulose involves a series of complex chemical reactions, including dehydration, depolymerization, and decarboxylation, resulting in the formation of a carbon-rich residue with a porous structure. For example, hard carbons (HC) produced from cellulose pyrolysis at temperatures between 700 and 1600°C were analyzed [64]. The alignment of graphene sheets above 1150°C resulted in larger micropores and a reduced Brunauer–Emmett–Teller (BET) surface area, while smaller crystalline domains formed above 1400°C. For samples pyrolyzed between 1300 and 1600°C, electrochemical tests in Na//HC cells showed a reversible capacity of 300 $mAhg^{-1}$ at C/10, effective cycling stability, and over 80% capacity retention at 5 C.

One of the main advantages of pyrolysis is its flexibility. Parameters like temperature, heating rate, and residence time can be precisely adjusted to customize the properties of the resulting carbon [65]. The gas environment and flow rate also significantly influence the quality of carbonization [66]. Additionally, post-treatment techniques, such as chemical and physical activation, can be employed to further enhance the surface area and pore distribution. Pyrolysis is highly scalable, thanks to adaptable reactor designs suitable for both laboratory and industrial production. Its modular setup allows multiple units to operate simultaneously, increasing overall throughput. Importantly, using cellulose as a renewable and plentiful feedstock ensures a sustainable and reliable supply, making pyrolysis an attractive method for producing functional carbon materials for postlithium energy storage [66].

3.1.1 | Slow Pyrolysis

Slow pyrolysis entails the gradual thermal decomposition of cellulose at a low heating rate, usually below 10°$Cmin^{-1}$, in an inert, oxygen-free atmosphere [67]. This method is shown to produce better deoxygenation, lower carbon yield, and chars with hydrophobic and graphitic properties, improved thermal stability, and functionalized surfaces on microcrystalline cellulose under a reductant N_2/H_2 atmosphere at intermediate temperatures (700°C), making them suitable for use in one-pot catalyst applications [67]. This heating condition typically involves controlled heating within a range of 400–800°C, with much longer residence times to ensure complete degradation of cellulose into stable carbon structures. This slow process helps preserve the original cellulose framework, which is why such carbon materials tend to have higher structural integrity and more defined porosity. For example, Shao et al. [68] studied the electrical conductivity of biocarbons derived from microfibrillated cellulose/lignosulfonate (MFC/LS) precursors during slow pyrolysis. Carbons were produced from MFC/LS blend precursors using slow pyrolysis at 0.2°C/min across a temperature range of 400–1200°C. The resulting carbons had low density (1.14 gcm^{-3}) and high electrical conductivity (95 S/cm) after pyrolysis at 1000°C [68].

One of the key benefits of slow pyrolysis is its ability to produce carbon with a well-developed porous network, which is helpful for energy storage applications. The slow heating rate promotes the gradual release of volatile components, leading to larger pore sizes and a more organized carbon structure compared to faster pyrolysis methods [69]. Additionally, this process helps retain certain functional groups that alter the surface chemistry of the carbon, enhancing ion transport and interactions in batteries or supercapacitors. Beyond structural benefits, this method allows adjusting pyrolysis conditions, such as temperature and time, to customize the carbon properties. Carbon produced at lower temperatures has higher oxygen content and lower conductivity, while higher temperatures yield more graphitic and conductive carbon. Furthermore, postpyrolysis activation with KOH or CO_2, along with steam treatment, enhances the surface area and porosity of the carbon [70].

3.1.2 | Fast Pyrolysis

Fast pyrolysis of cellulose-derived carbon involves a high heating rate, typically over 100°Cs^{-1}, with residence times under 2 s in an inert atmosphere or without oxygen. During this process, cellulose can quickly depolymerize and convert into carbon-rich materials. Operating within a temperature range of 450–700°C, this method rapidly breaks down cellulose into carbon-rich materials, bio-oil, and gaseous byproducts. Ye et al. [71] demonstrated that fast pyrolysis can produce activated carbon from various cellulose-based biomass sources. Among the three biomass materials—bagasse, poplar wood, and pine wood pine wood yielded the highest amount. It was highly selective due to its high volatile content and low ash content, which facilitates efficient thermal decomposition and conversion into bio-oil or char [72]. Additionally, Carrier et al. [73] argued that, together with mixtures of unlabeled and ^{13}C-enriched materials, fast pyrolysis microreactors and spectroscopic techniques, such as mass spectrometry and NMR spectroscopy, could provide a more comprehensive breakdown scheme for biomass fast pyrolysis, along with quantitative insights. Initially, controlling the pyrolysis regime was essential when choosing the reactor type for the process. As GC–MS has shown, secondary reactions are inevitable due to the chemical fragmentation patterns of "primary" fast pyrolysis volatiles. Using quantitative liquid-state ^{13}C NMR spectroscopy, the liquid fractions containing primary fast pyrolysis

condensates were analyzed to determine the quantitative distribution of functional groups. The origins of specific chemicals within the fast pyrolysis liquids were verified by compiling these findings into a map displaying the functional group distribution based on distinct and significant elements of the biomass [67].

Fast pyrolysis enables better control over the physico-chemical properties of cellulose-derived carbon by adjusting parameters such as temperature and heating rate [74]. Increasing the pyrolysis temperature can raise the level of carbonization, enhancing electrical conductivity in these materials. Additionally, optimizing feedstocks and reactor design can affect the yield and properties of the produced carbon. However, despite its advantages, fast pyrolysis may lead to lower structural integrity compared to slow pyrolysis, as rapid heating can cause carbon particles to become smaller and more disordered.

3.2 | Hydrothermal Carbonization

HTC of cellulose entails treating biomass in a water-rich environment at elevated temperatures (typically 180–250°C) and high pressure, thereby maintaining the water in its liquid state [75]. Under subcritical conditions, water serves as both a solvent and a reactant in the depolymerization of cellulose. During this process, glycosidic bonds are broken, resulting in the production of glucose and low-molecular-weight intermediates [75]. As these intermediates decompose through dehydration and decarboxylation, oxygen and hydrogen atoms are removed, which increases the carbon content of the solid residue.

The hydrochar yielded from the HTC of cellulose is rich in carbon and exhibits many desirable properties. Compared to untreated cellulose, it is usually more porous and has a greater surface area. Furthermore, it can be further modified with carboxyl (-COOH) and -OH functional groups [76]. Due to efficient carbonization during HTC, the carbon-to-oxygen ratio in the solid products is significantly higher than in untreated cellulose. Besides the solid hydrochar, HTC creates an organic liquid byproduct containing compounds such as acids, aldehydes, and furans, which can be recovered or further processed depending on the intended application. The HTC hydrochar displays unique properties suitable for energy storage, catalysis, and environmental cleanup. Its functionalized carbon structure allows it to adsorb various contaminants while maintaining oxygen-rich surface groups. Its porous structure also makes it useful in energy devices, like supercapacitors. In addition to the ability to adjust reaction conditions, the versatile HTC process enables the tailoring of material properties to maximize carbon content, surface functionality, or porosity [77]. Recent studies have investigated the effect of reaction parameters on the properties of HTC-derived carbon. For example, Volpe et al. [78] studied the reactivity of pure cellulose (CE) and birchwood (BW) under HTC conditions from 160 to 280°C, with a residence time of 0.5 h and a 1:5 biomass-to-water ratio. Thermogravimetric analysis (TGA) and Fourier-transform infrared (FTIR) spectroscopy elucidated how CE remained mostly unchanged below 220°C but experienced significant decomposition at 230°C, producing a thermally stable, aromatic-rich hydrochar. FTIR spectral analysis confirmed dehydration and aromatization reactions at temperatures ≥230°C. Meanwhile, BW hydrochars exhibited similar transformations only at temperatures ≥260°C, which is attributed to the protective effect of lignin in the plant matrix, thereby increasing thermal resistance.

HTC can also be used to enhance the energy storage capacity of carbon materials by doping heteroatoms. Research suggests a shift toward boric acid-based hydrochars, which introduce boron functionalities to improve the electrochemical performance and stability of the materials, as opposed to traditional precursors such as ammonium sulfate and thiourea. A heteroatom doping process that involves multiple atoms can be complex. In a study by Liu et al. [79], cellulose was subjected to HTC at 240°C for 1 h, using ammonium sulfate and thiourea as sources of inorganic and organic nitrogen, respectively, to produce supercapacitor carbon as shown in Figure 4. The effect of boric acid on the properties of hydrochar after KOH activation was examined, revealing that boric acid decreased functional groups and specific surface area and hindered micropore formation. In exploring the efficacy of hydrochar, specifically that synthesized from cellulose and organic nitrogenous compounds, a marked enhancement in both pore size distribution and electrochemical properties was observed after an activation process. Notably, when thiourea was used as the sole activating agent, the resultant hydrochar exhibited a surface area of 952.27 m^2g^{-1}. In a three-electrode system, the activated hydrochar displayed a specific capacitance of 235.8 Fg^{-1} at 1 Ag^{-1}, with a capacitance retention of 99.96% after 20,000 cycles at 10 A/g. These findings demonstrate the

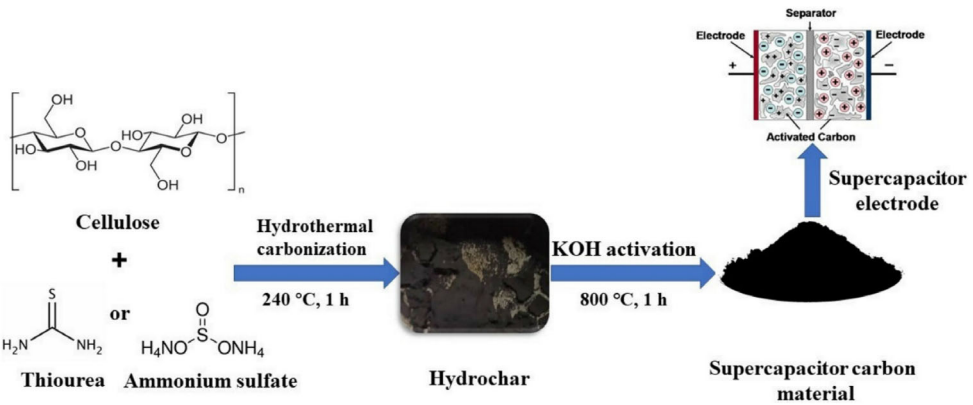

FIGURE 4 | Cellulose HTC with modifications of thiourea and ammonium sulphate. Copyright 2023, MDPI [79].

effectiveness of organic nitrogen compounds in producing high-performance supercapacitor carbon via HTC.

3.3 | Chemical Activation Methods

A well-established technique for enhancing the porosity and surface area of carbon materials, specifically those derived from cellulose, involves chemical activation. This method typically requires impregnating cellulose with particular chemical activating agents before its carbonization. Such impregnation helps establish a highly porous structure during the subsequent high-temperature treatment. Among the frequently utilized activating agents, KOH is prominent. In this established process, cellulose is saturated with KOH and then undergoes pyrolysis at temperatures between 600 and 900 °C, carried out in an inert atmosphere [70]. During pyrolysis, KOH decomposes and reacts with the carbon matrix, releasing gases, such as H_2, CO, and CO_2. These reactions form microporous structures by etching the carbon framework, significantly increasing the surface area and pore volume of the product. Phosphoric acid (H_3PO_4) is another commonly used activating agent. Cellulose is first impregnated with H_3PO_4 and then carbonized at temperatures ranging from 400 to 700°C [80]. H_3PO_4 promotes the depolymerization of cellulose, preventing the formation of tar and other by-products, and thereby leading to a higher carbon yield. Besides increasing porosity, H_3PO_4 adds phosphorus-containing functional groups to the carbon surface, which enhances hydrophilicity and improves both catalytic and adsorptive properties, making it especially useful for water treatment and electrochemical applications.

Zinc chloride ($ZnCl_2$) is another crucial activating agent for cellulose. The process begins with the addition of $ZnCl_2$, followed by heating to a temperature between 500 and 800°C. In this process, $ZnCl_2$ acts as a dehydrating agent, promoting the carbonization of cellulose and creating a network of mesopores and micropores. This method is well-known for producing highly porous carbons with a well-developed pore structure because of its interaction with $ZnCl_2$. Such a mature pore structure leads to carbons with high adsorption capacity, making them suitable for use in purification systems, catalysis, and electrodes for supercapacitors. For example, Bosch et al. [81] demonstrated that waste wood and biomass from forestry residues can be used as substitute feedstocks to produce activated carbon with $ZnCl_2$, with FTIR spectroscopy confirming oxygen-containing functional groups.

3.4 | Microwave-Assisted Carbonization

Microwave radiation-assisted carbonization of cellulose is a process in which cellulose materials decompose into carbon through rapid heating with microwave energy, as illustrated in Figure 5a. Cellulose is exposed to microwaves, typically in conjunction with a microwave-absorbing agent such as metal oxides or carbonaceous materials, which facilitates the efficient transfer of microwave energy to the biomass [84]. These absorbing agents enhance volumetric heating, ensuring that energy is evenly distributed throughout the material, rather than relying on external heat flux. This process enables faster and more energy-efficient carbonization compared to traditional thermal methods. Under inert conditions, cellulose degrades into carbon-rich material

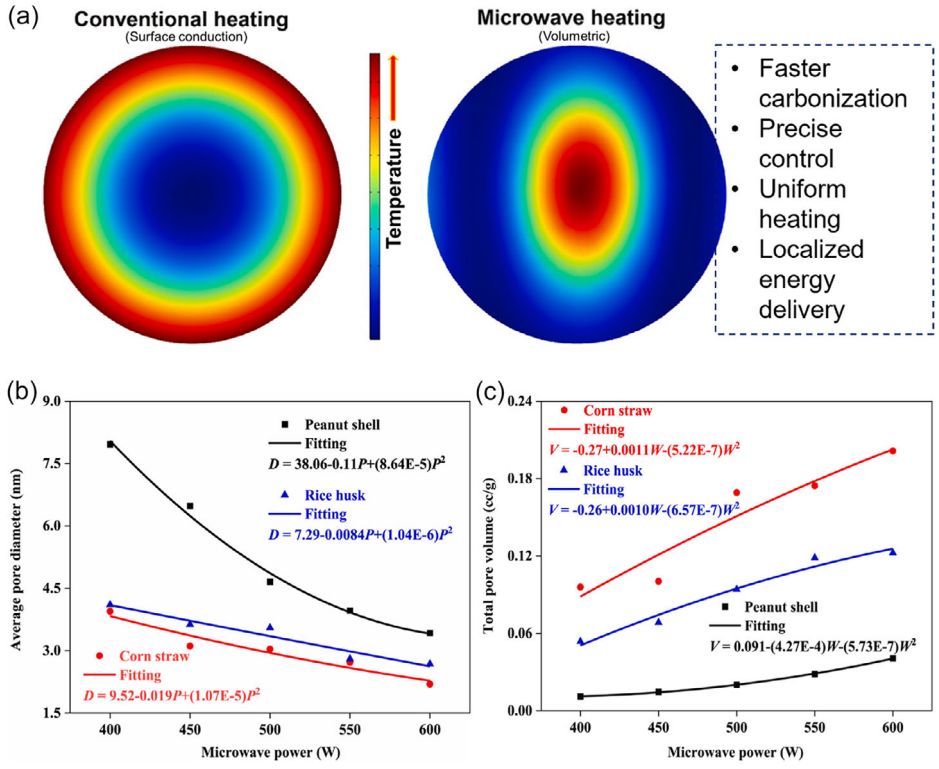

FIGURE 5 | (a) Schematic comparison of conventional and microwave heating (Copyright 2022, Elsevier) [82], and influence of microwave power on (b) average pore diameter and (c) total pore volume of the carbons obtained from cellulosic biomass sources (Copyright 2025, Elsevier) [83].

within minutes, making this technique highly time-efficient [85]. Besides its speed, microwave-assisted carbonization provides significant environmental benefits. It operates at lower temperatures and consumes less energy compared to traditional methods. Zhang et al. [62] examined how different process parameters affect the process and discovered that microwave heating speeds up the reaction by 5–10 times. This quick process also lowers the production of by-products like tar and toxic gases, making the process cleaner and more sustainable. Notably, the carbon often retains functional groups from the original cellulose, which can facilitate surface interactions and enhance performance in electrochemical applications.

Carbon materials created through microwave-assisted carbonization exhibit distinct physical and chemical characteristics. This is primarily due to the unusually rapid heating and precise control of decomposition that microwave technology facilitates during their production. As shown in Figure 5, a recent comprehensive study examined the microwave-assisted pyrolysis of three biomass: rice husk, peanut shell, and corn straw under variable microwave powers (400–600 W), pyrolysis temperatures (700–900°C), and residence times (60–180 min) [83]. The results showed a clear link between processing parameters and the structural properties of the resulting biocarbon. Specifically, increasing temperature, power, or time resulted in a gradual decrease in biochar yield, but a significant increase in porosity (Figure 5b,c). The specific surface area increased from 4.68 to 323.33 m^2g^{-1}, while the average pore diameter decreased from 16.55 to 2.19 nm, creating finer, more accessible pore networks.

In addition to process parameters, the choice of gas environment is crucial for determining the carbon quality. A recent study (Figure 6) introduced a cleaner pyrolysis strategy by combining microwave heating with catalytic treatment in a carbon dioxide (CO_2) atmosphere. Compared to conventional nitrogen environments, CO_2 significantly enhanced the porous structure and heating value of the resulting carbon while reducing gas yield [86]. The I_D/I_G ratio of the carbon decreased from 1.07 to 0.74 under CO_2, indicating a reduction in structural defects. Additionally, CO_2 improved the surface roughness and pore development of the biochar, making it more suitable for downstream applications. These findings on process parameters and the choice of gas environment demonstrate how precisely microwave-assisted pyrolysis can be specifically designed to produce carbon with specific pore structures, providing valuable guidance for designing high-performance carbon materials. Additionally, the ability to complete carbonization in a significantly shorter timeframe makes this method especially appealing for industrial-scale applications.

3.5 | Electrochemical Carbonization

Electrochemical carbonization is an emerging low-temperature method for transforming cellulose into carbon-rich materials

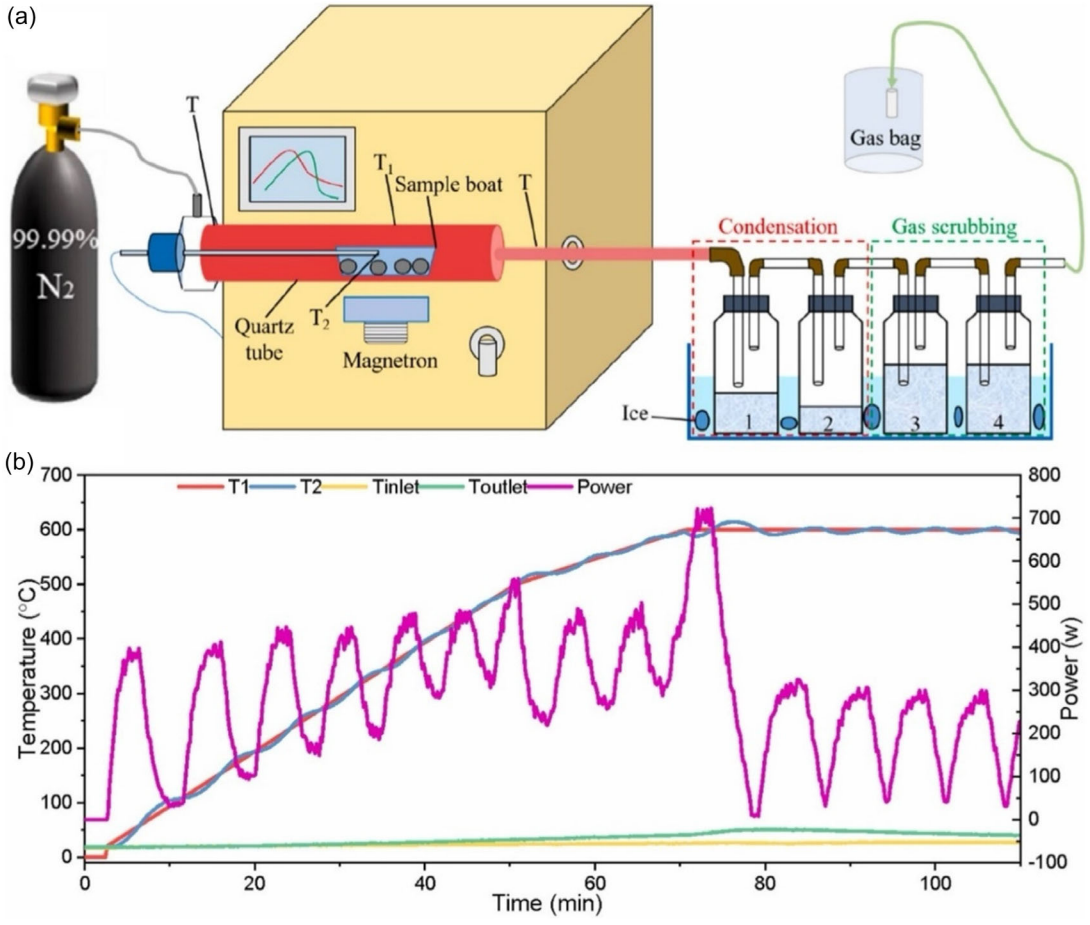

FIGURE 6 | Diagram (a) and thermal profiles (b) illustrating the process of microwave pyrolysis. Copyright 2024, Elsevier [86].

using electrical energy. A current is applied across electrodes as cellulose is immersed in an electrolyte solution. This process causes electrochemical oxidation and subsequent breakdown of the cellulose structure, primarily by removing hydrogen and oxygen atoms, resulting in a carbon-rich product [87]. Unlike conventional thermal carbonization, which relies on high temperatures, electrochemical carbonization operates at significantly lower temperatures, typically ranging from room temperature to ≈200°C. Using electric current for decomposition reduces the energy requirements and makes the process more environmentally friendly. Additionally, the structural and chemical properties of the resulting carbon can be precisely tailored by varying electrochemical parameters, including applied voltage, electrolyte composition, and reaction time.

In theory, such activation could involve electrochemical oxidation, doping, or structural modification to change the thermal degradation pathway of cellulose, thus enabling carbon creation at lower temperatures [88]. However, no comprehensive or scalable method has been established yet. Current research is limited to isolated proof-of-concept studies, which often focus on cellulose derivatives and are mostly confined to laboratory-scale experiments. These studies indicate the potential to modify the chemical structure of cellulose through electrochemical pretreatments or the use of rapid electrical heating methods, such as Joule heating. Nevertheless, these approaches do not yet provide a practical replacement for traditional high-temperature carbonization. Despite its promise, electrochemical carbonization remains in its early development stage and requires further investigation to achieve scalable, high-yield carbon production with properties suitable for specific energy storage applications.

The selection of a carbonization method for cellulose-derived materials largely depends on the desired structure–property relationship and the target energy storage application. Each technique (pyrolysis, hydrothermal, and chemical activation) offers specific advantages in controlling pore architecture, surface chemistry, and carbon ordering. For example, pyrolysis remains the most scalable route for producing porous carbons, while HTC enables the preservation of hierarchical structures and oxygen functionalities. Chemical activation, when optimized, enhances surface area and ion-accessible porosity, whereas microwave-assisted provides rapid, energy-efficient processing with tunable morphology at low temperatures. Rather than treating these methods as mutually exclusive, combining them strategically (e.g., hydrothermal pretreatment followed by activation) can yield carbons with synergistic textural and electrochemical properties. Ultimately, rational method selection should align with performance targets, such as conductivity, ion diffusion, or structural flexibility, rather than focusing solely on yield or cost. The following section discusses how these carbonization and activation routes translate into the fundamental structural, chemical, and electrochemical properties of cellulose-derived carbon materials, and how such parameters govern their suitability for various postlithium energy storage systems.

4 | Properties of Cellulose-Derived Carbon

The suitability of these carbon materials for postlithium energy storage depends on their ion storage behavior, cycling stability, and electrode–electrolyte interactions, which are directly determined by the morphology, crystalline structure (order), and surface chemistry (functional groups) of the carbon. These structural, chemical, and intrinsic properties are significantly influenced by the composition, molecular structure, and morphology of the biomass precursors, as well as the parameters of the carbonization process. Hence, this section discusses the properties and engineering strategies that support the development of advanced carbon materials from cellulosic sources, along with the essential tools for characterizing them.

4.1 | Optimal Chemical and Structural Characteristics for Carbonization

The structural and chemical characteristics of cellulose-derived carbons depend on the extent of carbonization, which can be monitored or analyzed using complementary analytical techniques that probe atomic structure, surface chemistry, and morphological features of carbon. First, the degree of carbonization, which indicates the transformation of cellulose into carbonaceous material, is commonly assessed using Raman spectroscopy, X-ray diffraction (XRD), and elemental analysis [89, 90]. Typically, the I_D/I_G ratio derived from Raman spectra, based on the peak intensities of the D-band (1380 cm^{-1}) and G-band (1595 cm^{-1}), provides information about the relative amount of disordered and graphitic carbon structures [91]. Furthermore, to track the level of carbonization, elemental microanalysis can be used to monitor the degree of carbonization and measure the carbon-to-oxygen (C/O) ratio, which serves as a measure of the progressive loss of oxygenated functionalities. Second, crystallinity and graphitization, which influence the electronic conductivity and structural stability of the carbon material, can be analyzed using XRD. The appearance of characteristic (002) graphitic peaks, indicating the formation of ordered carbon domains after carbonization, can be observed [89, 90]. Moreover, the interlayer d-spacing, which is crucial for the ease of alkali-ion (Na^+, K^+) intercalation and storage, can be measured using XRD. This can be further supported by high-resolution transmission electron microscopy (HRTEM), which reveals the ordered structure of carbon layers at the nanoscale. The expansion of d-spacing in hard carbons derived from cellulose enables the reversible insertion of larger ions, thereby enhancing cycling stability. Thirdly, the functional groups present after carbonization can be identified through FTIR and X-ray photoelectron spectroscopy (XPS) analyses, which analyze residual oxygen- or nitrogen-containing groups [92]. These functional groups are crucial for enhancing wettability, facilitating electrolyte penetration, and enabling surface redox activity, which is particularly beneficial for pseudocapacitive contributions in sodium- and potassium-ion storage.

Furthermore, microstructural features such as hierarchical porosity are crucial for enhancing ion accessibility and charge transport. The morphology and microstructure of the obtained carbon materials can be analyzed using scanning and transmission electron microscopies (SEM/TEM). Then, porosity and surface area, which determine the capacity for ion transport and charge storage, can be quantified by BET analysis [93]. The presence of micro- and mesopores enhances the electrode–electrolyte interface, increasing ion accessibility and facilitating rapid

electrochemical reactions. Tuning the pore size distribution through activation or templating strategies is essential for optimizing rate performance and capacity retention. As it is, a balance between graphitization and porosity must be maintained to ensure both electrical conductivity and enough active sites for ion storage. These techniques reveal the retention of fibrous structure, pore development, and surface roughness, all of which affect electrode–electrolyte interactions and mechanical stability. As a result of controlled carbonization, the intrinsic properties, such as electrical conductivity, mechanical stability, and thermal stability, determine the functional performance of carbon electrodes, especially in postlithium energy storage systems.

4.2 | Electrical Conductivity

The electrical conductivity of cellulose-derived carbon is primarily influenced by its microstructure, which is shaped during the carbonization process. During thermal treatment, cellulose is transformed into a carbonaceous material with a microcrystalline structure, a key feature that facilitates electron transport [94]. In this regard, even the degree of graphitization, porosity, and carbon surface area is critical in assessing conductivity. Graphitization typically increases with higher carbonization temperatures, resulting in enhanced conductivity due to the formation of more ordered carbon domains that facilitate efficient electron mobility. Additionally, the presence of micropores and mesopores enhances electron transfer pathways, further contributing to the overall conductivity of the material, which is particularly beneficial for energy storage applications.

Gelfond et al. [94] reported the preparation of highly conductive carbon fibers from biomass, as shown in Figure 7. They demonstrated that high electrical conductivity carbon produced from bamboo cellulose can sequester 0.85 tons of carbon per hectare of bamboo annually. Air-drying and performic acid treatment were used to isolate microfibers from bamboo cellulose. After stabilization and carbonization, conductive carbon fibers were produced. The carbon fibers were joule-heated for 20–30 s at 2000°C to create graphitized carbon fiber. The resulting carbon fibers exhibited one of the highest electrical conductivity values among biomass-derived carbon fibers, measuring 25,300 ± 6,270 Sm^{-1}, and showed perfect alignment of nanofibrils [94].

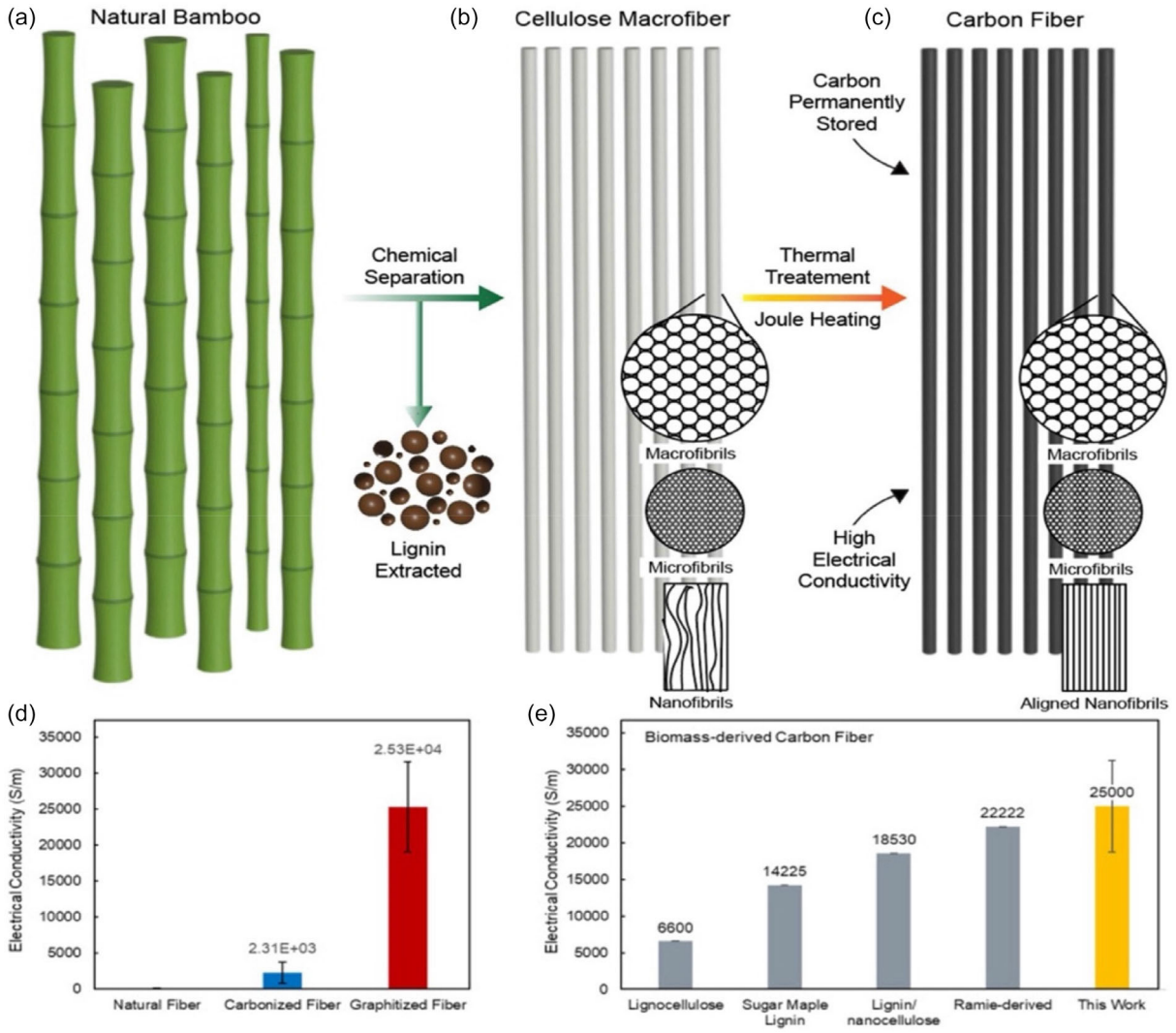

FIGURE 7 | A schematic illustrating the production of highly conducting cellulose-derived carbon fibers derived from bamboo (a–c), and benchmarking of the obtained electrical conductivity of various biomass-derived carbons (d,e). Copyright 2023, Elsevier [94].

The inclusion of heteroatoms, such as nitrogen, sulfur, or phosphorus, significantly enhances the conductivity of biomass-derived carbon. For instance, nitrogen doping creates defects in the carbon lattice that facilitate electron movement, thereby increasing electrochemical performance by creating more active charge storage sites. Conducting polymer particles based on N, P, and S had similar effects on the electronic structure of carbon, thus increasing overall conductivity. These dopants not only improve intrinsic conductivity but also enhance the material-solvent interface in electrochemical devices [95]. Therefore, cellulose-based carbon materials containing heteroatoms have better conductivity than those without.

4.3 | Mechanical Properties

Mechanical integrity and structural stability are supported by the fibrous microstructure inherited from the native cellulose structure, including hierarchical porosity and preserved morphology, which enhances mechanical strength in derived carbon frameworks [45, 46, 96]. Materials such as carbon nanofibres and aerogels, templated from nanocellulose precursors, demonstrate high structural integrity and resilience when subjected to cycling or mechanical stress [97, 98]. The retention of connected fiber networks also minimizes particle pulverization, preventing loss of electrical contact during electrode expansion and contraction cycles.

The carbon materials obtained often exhibit good mechanical stability and resilience, especially those produced at higher temperatures, since increased carbonization and graphitization enhance structural integrity. For example, Sporl et al. [99] showed that using ammonium tosylate as a sulfur-based carbonization agent at 1400°C significantly increased the tensile properties of cellulose-derived carbon fibers, with a carbon yield of 37% (83% of the theoretical maximum), tensile strength of 2.0 GPa, and Young's moduli reaching 84 GPa. Similarly, Vocht et al. [100] applied a pressure-assisted stabilization method to produce carbon fibers from cellulose as commercial tire cord fibers (TC-P) and air gap-spun cellulosic fibers (HC-P). The stabilized fibers were continuously carbonized at 1400°C in a laboratory setting. Carbon fibers generated exhibited tensile strengths of 2.8 GPa and Young's moduli of 112 GPa. However, mechanical performance can vary significantly depending on porosity and surface defects. While high porosity enhances properties such as adsorption and ion transport, which are crucial for energy storage, excessive porosity can compromise mechanical strength, resulting in brittleness and fracture under stress. To address this, cellulose-derived carbon can be reinforced by blending with polymers or metal oxides, which improves mechanical integrity without sacrificing electrochemical performance. This balance is particularly important in applications such as supercapacitor electrodes and electrocatalysts, where mechanical durability and conductivity are required. Therefore, for highly reliable and long-term performance of advanced energy storage systems, it is essential to optimize the mechanical properties of cellulose-derived carbon [101].

4.4 | Thermal Properties

Carbon derived from cellulose can offer higher thermal conductivity due to increased graphitization and better alignment of the carbon layers, allowing heat to transfer more easily within the material [102]. Higher carbonization temperatures promote the formation of graphitic domains, thereby increasing crystallinity and reducing structural defects. This ordering enhances thermal resistance by reducing the number of sites susceptible to degradation at high temperatures. Consequently, cellulose-derived carbon usually shows decomposition resistance above 600°C in inert atmospheres [103].

The thermal behavior of cellulose-derived carbon can also be influenced by surface functional groups, including -OH, -COOH, and oxygen-containing species. While these groups increase chemical reactivity, they create thermally unstable sites prone to oxidation or decomposition at high temperatures [104]. Therefore, postcarbonization chemical treatments for activation, such as KOH or H_3PO_4, may modify or remove these groups, thereby further improving thermal stability. Additionally, heteroatom doping, such as nitrogen or boron, strengthens the carbon lattice in cellulose-derived carbon, enhancing its resistance to thermal degradation and oxidation at high temperatures.

The porous structure and surface morphology of the material also influence its performance in high-temperature environments. Increased graphitization and better alignment of carbon layers can enhance thermal conductivity, enabling more efficient heat dissipation within the material [104]. However, the presence of amorphous regions, structural defects, and phonon-scattering sites in cellulose-derived carbon generally keeps its conductivity lower than that of fully graphitized materials, such as graphite. Overall, the interplay between crystallinity, surface chemistry, and morphology determines the thermal durability and conductivity of cellulose-derived carbon, allowing these materials to be tailored for demanding applications where both stability and functional performance are essential.

4.5 | Tunability of Structural Properties

The physical properties of cellulose-derived carbon are determined by the carbonization process and the inherent structure of cellulose [105]. For example, the mechanical integrity of cellulose and the specific conditions of the carbonization process contribute to the robustness of the resulting carbon structure. Although lightweight, cellulose-derived carbon can still maintain significant structural strength, especially when preserving the original fiber network. As shown in Figure 8, the structural properties of cellulose-derived carbon stem from the hierarchical architecture of cellulose precursors. During carbonization, the fibrous morphology of cellulose is partially retained, resulting in a porous, interconnected carbon network comprising crystalline and amorphous regions. Moreover, the degree of crystallinity of native fibers increases with higher carbonization temperatures and more rigorous processing conditions.

The carbonization of pretemplated or prewoven cellulose precursor structures also helps to prepare carbon in sheet, woven, and porous membrane structures. For example, Kuzmenko et al. [112] introduced novel, environmentally friendly fiber materials from cellulose that can be used as supercapacitor electrodes. To create a composite CNF/carbon nanotube (CNT) electrode, vapor-grown CNTs were applied to nanofibrous carbon nanofiber mats. Compared to pure carbon nanofibers, the resulting composite

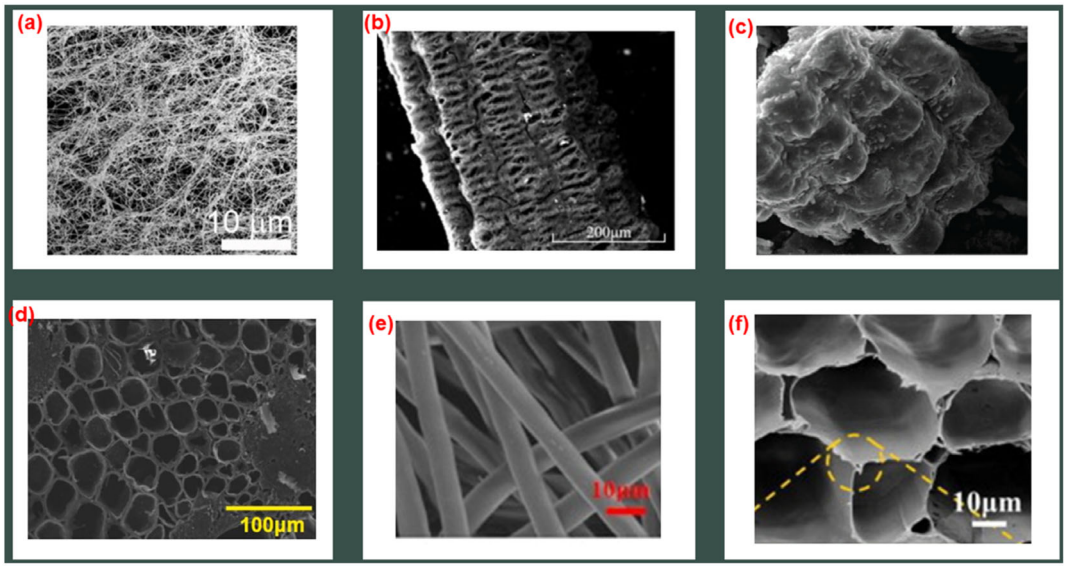

FIGURE 8 | SEM images of various porous and carbon structures of cellulose in (a) bacterial cellulose. Copyright 2021, Elsevier [106], (b) rice husk. Copyright 2022, Elsevier [107]. (c) peanut shell. Copyright 2023, Tech Science [108], (d) bamboo. Copyright 2024, Elsevier [109], (e) cotton. Copyright 2018, Elsevier [110], and (f) wood. Copyright 2021, Elsevier [111].

exhibited significantly higher conductivity and a substantially larger surface area. Furthermore, Jayamani et al. [113] noted that the physical properties of the carbon structures derived from cellulose can vary depending on how they are woven or applied. The surface area ranges from a few hundred to over a thousand square meters per gram, depending on the activation method. This distribution results from a porous structure composed of micropores (<2 nm), mesopores (2–50 nm), and occasionally even macropores (>50 nm) [105]. This distinct porosity profile is well-suited for applications in adsorption, catalysis, and energy storage. The porosity can be adjusted through various activation processes, including chemical activation with KOH or physical activation with gases such as CO_2 or steam, to tailor the material for specific uses, such as electrode materials in supercapacitors and batteries. Besides porosity, bulk density and particle size are important physical properties of cellulose-derived carbon that affect its performance. These carbons typically have low bulk density due to their high porosity, making them lightweight and beneficial for applications [114]. Particle size control can be easily achieved through grinding or milling after carbonization. This influences how the carbon material interacts with fluids or electrolytes in energy storage devices. Moreover, carbon materials generally appear black and odorless, with excellent dispersibility in various matrices, especially when functionalized or doped with heteroatoms. All these physical properties, combined with their renewable and biodegradable origin, make cellulose-derived carbon a versatile material for energy-storage applications [115].

Overall, by controlling carbonization parameters, such as temperature, activation method, and precursor morphology, key attributes, including porosity, interlayer spacing, graphitization degree, and surface functionality, can be tailored to optimize ion transport, conductivity, and mechanical resilience. For instance, expanded interlayer spacing and hierarchical porosity facilitate the accommodation of larger ions (Na^+, K^+, Mg^{2+}, and Zn^{2+}), while heteroatom doping (N, S, P, and B) introduces redox-active sites and enhances electronic conductivity. The balance between amorphous and graphitic domains, along with the retention of functional groups, is essential for achieving high capacity, rate performance, and cycling stability. Hence, cellulose serves not only as a renewable feedstock, but also as a programmable scaffold (from nanocrystals to aerogels or films), enabling the rational design of carbon architectures tailored for specific electrochemical functions.

5 | Applications of Cellulose-Derived Carbon in Postlithium Energy Storage Technologies

Cellulose-derived carbon is widely used in various energy storage technologies beyond lithium, including, but not limited to, SIBs, KIBs, ZIBs, supercapacitors, and hybrid energy storage systems [116]. For instance, sodium-ion and KIBs utilize electrode materials that exhibit high capacity, excellent cycling stability, and efficient ion transport due to their tunable porosity and carbon arrangements, in addition to a high surface area [117]. The carbon derived from cellulose generally exhibits stable electrode performance in ZIBs because of its structural flexibility and electrochemical stability in aqueous electrolytes. Additionally, it also plays a significant role in supercapacitors by enhancing both power and energy density, owing to its fast charge–discharge capability and large surface area. Furthermore, further functionalization of cellulose-derived carbon with functional groups or dopants opens up a spectrum of applications, including the potential to tailor properties for specific storage technologies beyond conventional lithium-ion systems [118].

5.1 | Sodium-Ion Batteries (SIBs)

High-surface-area carbon derived from cellulose significantly improves SIB performance, offering excellent pore structure tunability and originating from a sustainable source [119]. Therefore, the value of cellulose-derived carbon as an electrode is significant for SIBs because the relatively large ionic radius

of sodium ions (Na^+) exceeds that of lithium ions (Li^+). Cellulose-derived carbon, with its highly porous structure, provides sufficient space for Na^+ diffusion and storage, thereby reducing the risk of electrode degradation from the repeated insertion and extraction of sodium ions [120]. Additionally, hierarchical porosity, ranging from micro- to mesopores, enhances ion transport pathways, facilitating faster kinetics and improved rate capability in SIBs. Carbonization conditions dictate the electrochemical characteristics of cellulose-derived carbon in SIBs. The degree of graphitization is notably higher when cellulose-derived carbon is pyrolyzed at high temperatures, resulting in improved electrical conductivity, which is the most crucial factor for the performance of a Na-ion battery. Conversely, lower-temperature pyrolysis leaves oxygen-containing functional groups on the carbon surface, which can enhance the interaction between Na^+ and the carbon, resulting in increased reversible electrode capacity. Maintaining a balance between a graphitic structure and retaining functional groups is crucial for achieving optimal charge storage and high cycling stability in cellulose-derived carbon for SIBs [121].

Notably, the potential of bio-derived nanoscale carbon materials in enhancing the performance of SIBs has been demonstrated [122–124]. A hard carbon was prepared from nanocellulose extracted from Spinifex grass (*Triodia pungens*) after minimal pulping and carbonization [125]. The resulting carbon anode exhibited an exceptional capacity for SIBs of 386 $mAhg^{-1}$, attributed to its significant interlayer spacing (≈0.39 nm), facilitating sodium-ion storage [126]. The material also demonstrated exceptional cycling stability and rate capability, valuable for potential next-generation battery applications. For sodium ions to be accessible and stored effectively, carbon structures at the nanoscale must be optimized, mainly through the control of interlayer spacing and defect engineering. In this pathway, several studies have focused on deconstructing cellulosic sources into nanomaterials as precursors for carbon electrode materials, including the use of a microbial-chemistry-assisted approach to tailor the resulting microstructure [127, 128].

Chemical pretreatments and activation in general enhance surface area and pore volume, specifically increasing sodium storage capacity. In our recent work, we have demonstrated that chemical pretreatment of lignocellulosic biomass can be effectively employed to tailor the chemical composition and morphological features of hard carbons for SIB storage. Using sugarcane biomass as a feedstock, we have applied three distinct chemical pretreatments to selectively adjust the proportions of lignin, cellulose, and hemicellulose before direct carbonization (Figure 9). This strategy has enabled precise control over porosity

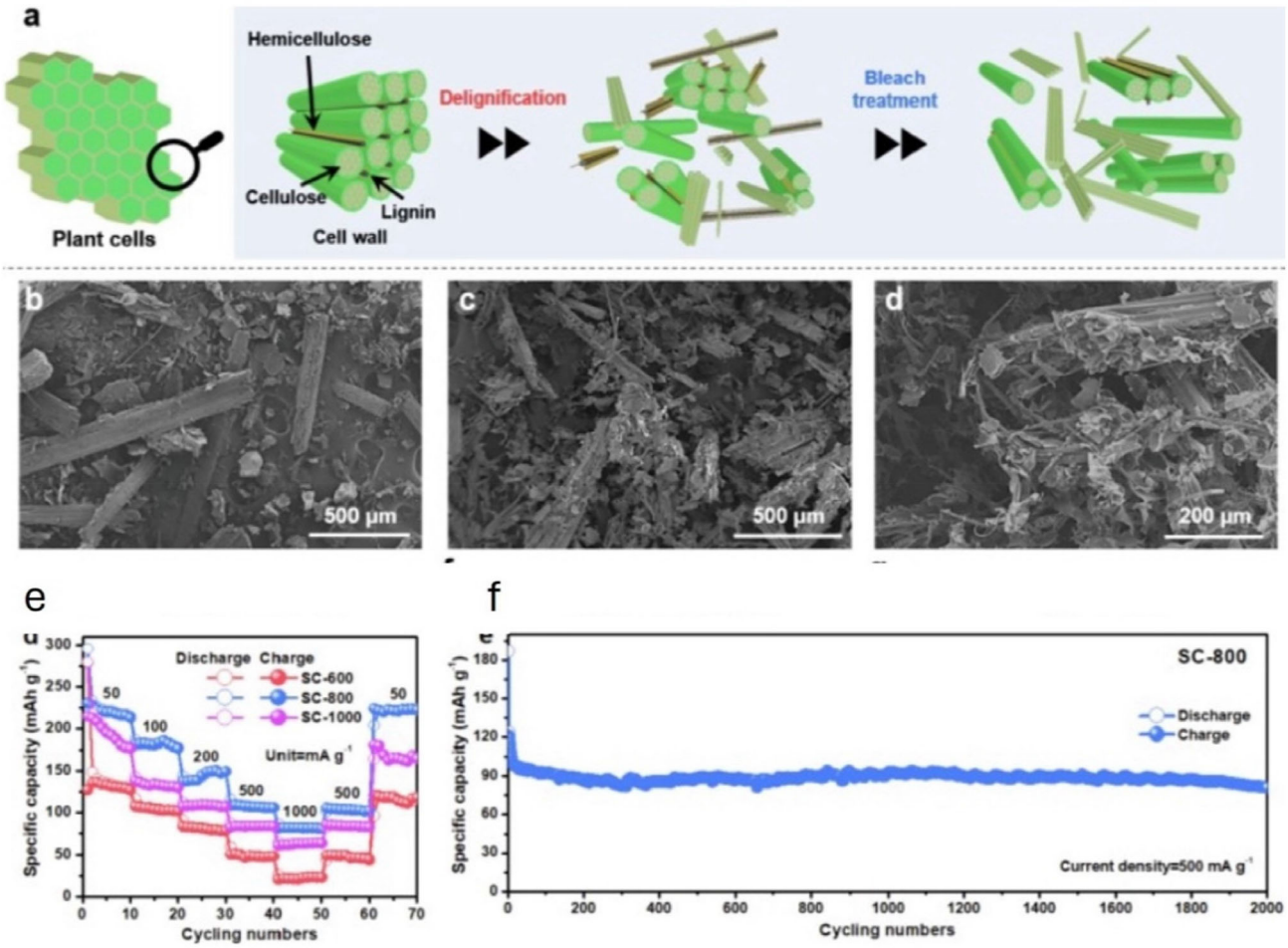

FIGURE 9 | Schematic workflow and electrochemical performance of chemically pretreated sugarcane biomass-derived carbon anodes for sodium-ion storage. (a) Schematic of delignification, (b–d) SEM image of sugarcane biomass) showing the gradual changes in morphology, (e,f) rate performance, and cycling stability of bleached sugarcane annealed at various temperatures (e) and 800°C (f). Copyright 2022, Elsevier [129].

and structural features, which are critical for efficient Na^+ adsorption and intercalation. The optimised carbon anode initially delivered a reversible capacity of 229 $mAhg^{-1}$. It maintained 189 $mAhg^{-1}$ at 100 mAg^{-1} after 50 cycles, with an unusually low discharge voltage plateau below 0.5 V contributing ≈74% of the total capacity. The corresponding relative energy density has reached 500 $Whkg^{-1}$ in the first cycle and has remained at 416 $WhKg^{-1}$ after 50 cycles. Remarkably, the material has exhibited ultrastable cycling, showing almost no capacity fading over 2000 cycles [129]. Minimal volumetric change during *sodiation and desodiation*, confirming that chemical optimization of the lignocellulosic composition imparts a robust structural framework capable of sustaining repeated Na^+ insertion and extraction. These findings have underscored our approach of using chemical pretreatment to tune both the composition and morphology of biomass-derived carbons, achieving long-life, high-energy, and low-cost anodes for SIBs [129].

Our group further demonstrated the influence of heteroatom doping as a powerful strategy to enhance the sodium storage capability of cellulose-derived and other biomass-based hard carbons by simultaneously modulating their structural and electronic properties. Codoping with nitrogen and sulfur, as demonstrated in nanosheet-like sorghum biomass-derived carbons, introduces abundant defect sites and heteroatom-rich functional groups that serve as additional Na^+ adsorption centers while also expanding the interlayer spacing to facilitate reversible intercalation [130]. Optimizing the carbonization temperature is crucial for balancing heteroatom retention and graphitization, as studies have shown that moderate temperatures (e.g., 600°C for N, S codoped sorghum carbons) maximize reversible capacity and conductivity. These materials have delivered reversible capacities exceeding 250 $mAhg^{-1}$ and remarkable cycling stabilities, attributed to enhanced pseudocapacitive contributions, improved surface wettability, and stable solid–electrolyte interphase (SEI) formation. Density functional theory (DFT) calculations further confirmed that N and S dopants reduced the Na^+ adsorption energies and increased binding site densities, underscoring the mechanistic basis for improved ion storage.

In this context, nitrogen-doped carbon serves as a good example, where incorporating nitrogen into the carbon matrix introduces defects that act as extra active sites for Na^+ storage, boosting overall capacity and charge–discharge efficiency. Conversely, phosphorus doping improves structural integrity, thereby reducing the typical volume expansion associated with sodium insertion. These doping strategies can also enhance the electronic conductivity of cellulose-derived carbon, resulting in improved rate performance and increased cycling stability for long-term use. N/S-doping is an alternative to N-doping for improving conductivity and electrochemical performance. Xu et al. [117] developed hierarchical N/S codoped carbon microspheres, which are pyrolyzed composite microspheres composed of cellulose/polyaniline (PANI). The microsphere shape enables the current collector and active materials to adhere more effectively, while a nanosized, interconnected wall provides electron pathways and shortens the Na^+ diffusion distances. However, the composite interface might hinder charge transfer due to charge buildup.

Further, deconstructing cellulose into CNCs provides a highly uniform, nanoscale precursor that translates into carbon with finely tunable structural properties for sodium-ion storage. In a recent study, CNCs were observed to offer a large specific surface area and a well-defined rod-like morphology, enabling the derived carbons to exhibit hierarchical porosity and an expanded interlayer spacing, both of which are critical for accommodating larger Na^+ ions (compared to lithium) through combined adsorption and intercalation. As shown in Figure 10, electrochemical testing of Na-metal half-cells confirms that the sodium storage behavior of these carbons is strongly structure-dependent. Carbons produced at moderate carbonization temperatures (≈1500°C) achieve an optimal balance: sufficient surface area to promote reversible sodium uptake, yet a level of structural ordering that limits excessive SEI formation and capacity loss. While high-surface-area carbons enhance both reversible and irreversible capacities, their continuous SEI growth during cycling leads to pronounced capacity fading. CNC-derived carbons thus provide a pathway to engineer carbon materials with tailored porosity, controlled graphitic ordering, and optimized surface chemistry, resulting in improved reversible capacity and cycling stability in SIBs [131].

Codoping with N/S boosts sodium storage and rate capacity by increasing the distance between carbon layers, raising the Fermi level, and enhancing the electronic conductivity of the material. Anode materials with high-rate capacity benefit from S-doping, as it increases their electronegativities and electrochemical activities [132]. Introducing S atoms into the sp^2 carbon framework forms sulfur species such as thiol, thiophene, and sulfonic acid. Jin et al. [133] pyrolyzed BC at 800°C and combined it with S at 500°C in Ar, yielding 15 wt% S-doped carbon nanofibers (S-CNF). These delivered 257 $mAhg^{-1}$ at 8 $A\,g^{-1}$, with improved Na^+ storage due to nanovoids, defects, and S-doping. S-doping reduced the bandgap, enhancing conductivity, while P-doping further improved charge transfer and Na^+ adsorption through stronger electron donation and bonding [134]. The P—C bond length results in a pyramidal shape, disturbing the carbon plane and creating an open-edge morphology. Phosphorus doping initially introduces unstable states that oxidize over time. Tao et al. [135] synthesized N, P dual-doped hollow carbon fibers/graphitic C_3N_4, achieving 93 $mAhg^{-1}$ at 5 Ag^{-1} and 280 $mAhg^{-1}$ at 0.1 Ag^{-1}, supported by a conductive network. Boron (B) doping enhances Na^+ interaction by acting as an electron acceptor, thereby improving diffusion dynamics. In contrast, F doping lowers the energy barrier for Na^+ inclusion [136]. However, there is no existing literature on F-doped carbon derived from cellulose precursors.

After pyrolysis, cellulose-based materials retain their natural structure and are capable of anchoring active nanoparticles. However, they do not conduct electrons well. Charge transfer in cellulose-derived carbon can be enhanced by combining conductive materials. The internal structure and composition of carbon electrodes influence reaction rates and transfer processes. Shi et al. [137] utilized graphene to initiate microwave-assisted carbonization of CNF, resulting in a material with a discharge capacity of 558 mAh/g and rate performance of 100 mAh/g at a current density of 3.2 Ag^{-1}. Combining cellulose precursors with metal–organic frameworks (MOFs) enables a continuous charge–transfer mechanism, thereby enhancing charge transport. Li et al. [138] synthesized Co_3O_4@N doped carbon nanofibers (N-CNFs), a porous electrode with embedded Co_3O_4 nanoparticles, through in situ growth and pyrolysis,

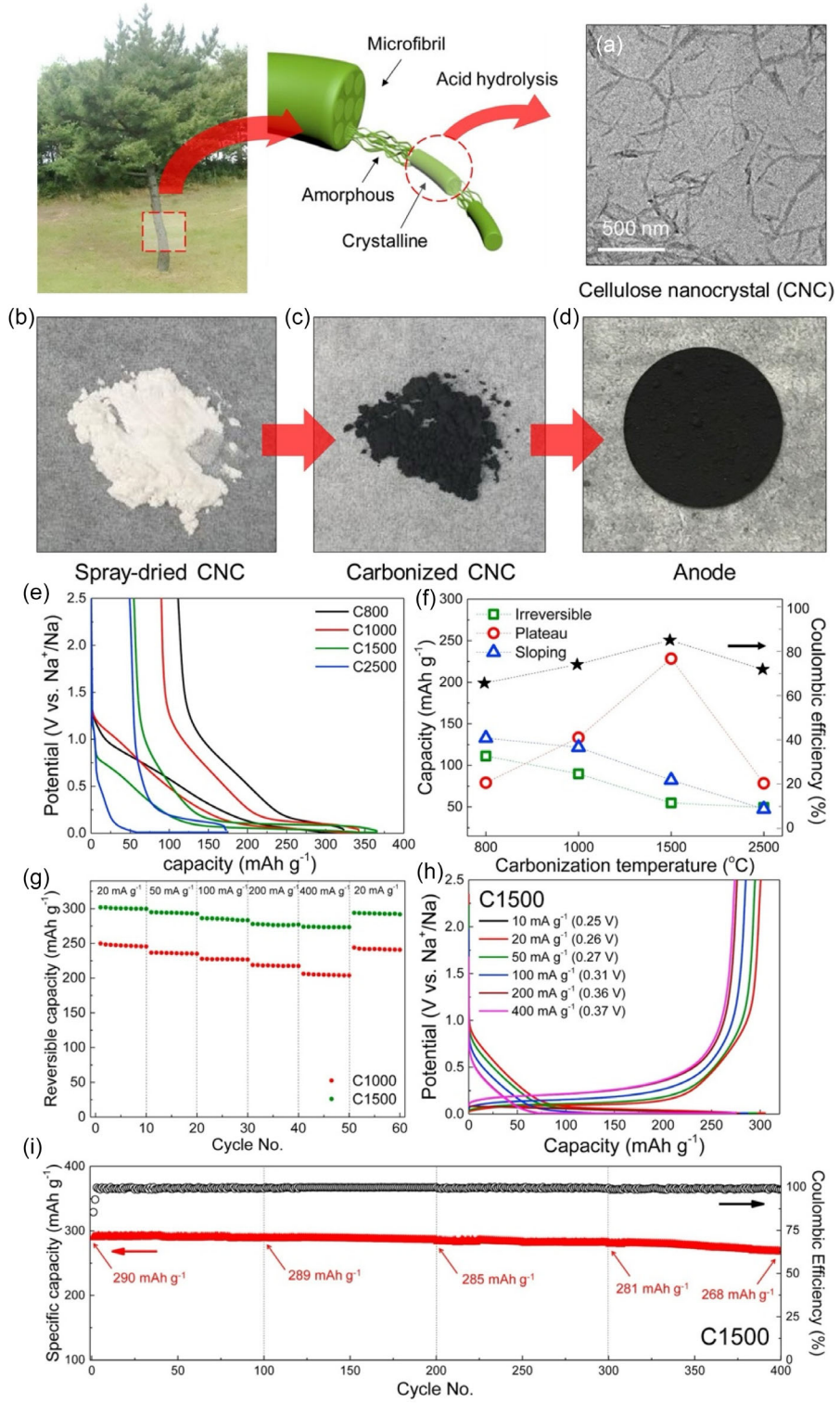

FIGURE 10 | Schematic workflow and electrochemical performance of CNC-derived carbon anodes for sodium-ion storage. (a) TEM image of CNCs showing their uniform rod-like morphology, obtained by deconstructing natural cellulose. (b–d) Photographs of spray-dried CNC powder, carbonized CNCs, and the fabricated CNC-derived carbon anode coated on Cu foil. The electrochemical properties were normalized to the mass of CNC in the electrode. (e) First galvanostatic charge–discharge profiles of CNC-derived carbon anodes at 10 mA/g. (f) Breakdown of irreversible capacity, sloping capacity (>0.2 V), plateau capacity (<0.2 V), and coulombic efficiency as functions of carbonization temperature, derived from (e). (g) Rate performance of CNC carbons over 20–400 mAg^{-1}, with C1500 exhibiting the highest reversible capacity (273 $mAhg^{-1}$ at 400 mAg^{-1}). (h) Voltage profiles of C1500 at different current densities, demonstrating minimal capacity fading and a stable low-voltage plateau. Values in parentheses denote average oxidation voltages. (i) Cycling stability and coulombic efficiency of C1500 at 100 mAg^{-1} over 400 cycles, confirming sustained capacity retention and >99% coulombic efficiency. Copyright 2020, Elsevier [131].

resulting in high rate capability and a discharge capacity of 205 $mAhg^{-1}$ at 3,200 mAg^{-1}. Adding metal nanoparticles, including Co_3O_4, Fe_3O_4, CuO, and ZnO, to cellulose-based composites increases their performance. He et al. [139] demonstrated that combining hard and soft carbon enhances electrochemical performance by coating soft carbon on hard carbon, which improves rate capacity by decreasing SEI formation and oxygen-containing defects. Hence, improved capacity and rate performance in carbon materials can be achieved by using hard and soft carbon.

Furthermore, cellulose-derived carbon shows promise as a composite material with other active substances in SIBs. By combining cellulose-derived carbon with metal oxides or sulfides, the synergistic enhancement of sodium storage capacity and cycling performance can be achieved. The carbon matrix provides conductive support to buffer the volume changes of metal-based active materials during sodiation-desodiation processes, thereby improving the mechanical integrity of the electrode. Poly(methyl methacrylate) (PMMA), known for its ease of processing and adjustable porosity, is often used to produce cellulose-derived carbon. Wang et al. demonstrated a method for combining BC and PMMA to form 3D porous composites through thermally induced phase separation. PMMA pyrolysis created micro- and mesopores, enabling better Na^+ diffusion

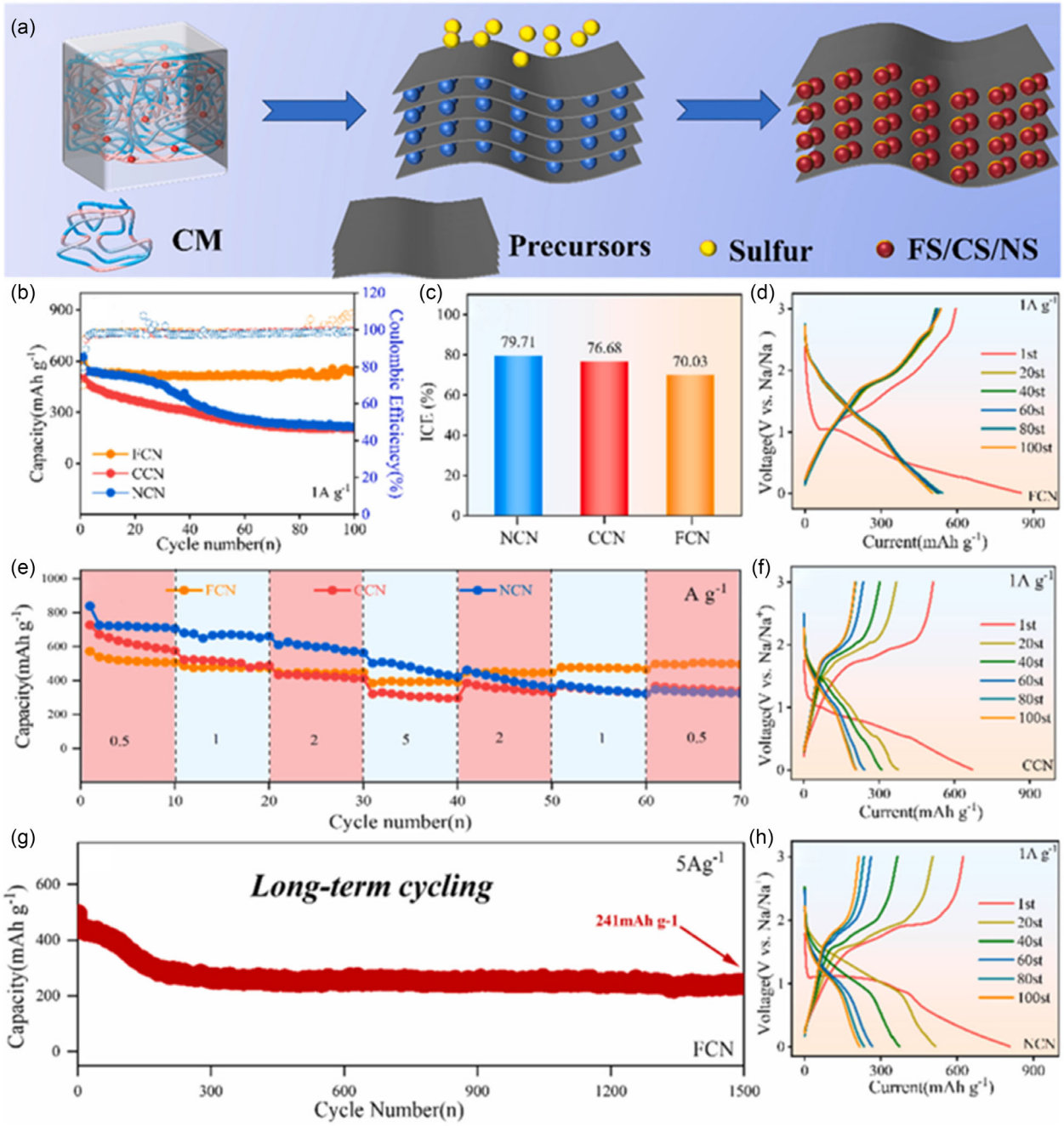

FIGURE 11 | (a) Schematic for the preparation of metal sulfide carbon composites; (b) cycling stability at a current density of 1 Ag^{-1}; (c) comparison of initial coulombic efficiency; (d) galvanostatic charge discharge of FCN, (f) CCN, and (h) NCN; (e) rate capability at various current densities; and (g) long-term cycling stability. Copyright 2025, Elsevier [142].

and a capacity of 380.66 $mAhg^{-1}$ at a current density of 0.03 Ag^{-1} [140]. BC ensured a stable conductive network, enhancing rate performance. Wang et al. used unidirectional ice templating to prepare vertically aligned carbon aerogels, which showed lower charge transfer resistance due to their distinctive honeycomb microstructure [141]. Merging cellulose with polymers helps develop stable conductive networks and customizable ion channels, although controlling the detailed carbon structure remains challenging.

In another study by Chen et al. [142] transition metal sulfides, such as FeS_2 (FCN), CoS_2 (CCN), and NiS_2 (NCN), uniformly dispersed on carbon layers from carboxymethyl cellulose, were evaluated as anode materials for SIBs (Figure 11a). The study found that optimizing metal cations improved crystallinity and particle uniformity, with FCN exhibiting the best Na^+ diffusion, cycling stability, and fast charge/discharge, delivering 536 $mAhg^{-1}$ at a current density of 1 Ag^{-1} after 100 cycles (Figure 11b). Although FCN showed a lower initial coulombic efficiency of 70.03% due to electrolyte decomposition and SEI formation (Figure 11c,d,f,h) from its high surface area, it achieved an initial charge capacity of 594.2 $mAhg^{-1}$ and a discharge capacity of 850.7 $mAhg^{-1}$, due to the presence of nitrogen heteroatoms and the presence of C—S bonds. Electrochemical analysis revealed that the charge storage in FCN was dominated by pseudocapacitive behavior, with pseudocapacitive contribution increasing with scan rate, reaching 90.82% at 0.9 $mVs^{-1.}$ Despite limited Na^+ diffusion at high scan rates, FCN maintained good rate capability and reversibility, retaining 241 $mAhg^{-1}$ at a current density of 5 Ag^{-1} after 1500 cycles, outperforming most reported iron sulfide-based anodes (Figure 11e,g). This approach is scalable and has the potential to be adaptable to other chemistries, which could accelerate the development of cost-effective, high-power SIBs for grid and large-scale energy storage applications.

TABLE 2 | Role of structural parameters, properties and morphologies of cellulose-derived carbon in various postlithium energy storage technologies.

Carbon material property	Structural/ functional role	Sodium-ion batteries (SIBs)	Potassium-ion batteries (KIBs)	Magnesium/Zinc-ion batteries (MIBs/ ZIBs)	Supercapacitors
Surface area	Provides active sites for ion adsorption	Enhances Na^+ storage and rate capability	Improves K^+ accessibility and charge/discharge rates	Facilitates Zn^{2+}/Mg^{2+} adsorption and uniform deposition	Boosts capacitance via double-layer formation
Porosity (Micro/ Meso/Macro)	Enables ion transport and electrolyte access	Hierarchical pores improve Na^+ diffusion and cycling	Mesopores accommodate large K^+ ions; micropores store charge	Prevents dendrite formation in ZIBs; buffers Mg^{2+} volume changes	Enhances ion diffusion and charge storage kinetics
Interlayer spacing	Reduces ion diffusion barriers	Expanded d-spacing allows reversible Na^+ intercalation	Turbostratic disorder supports K^+ insertion with minimal strain	Facilitates Mg^{2+} intercalation; stabilizes Zn^{2+} storage	Not critical but may aid hybrid systems
Graphitization degree	Improves conductivity and structural integrity	Semi-graphitic carbons balance conductivity and capacity	Graphitic domains enhance K^+ transport and cycle life	Improves electron transfer and suppresses passivation	Enhances conductivity for fast charge/discharge
Surface functional groups (–OH, –COOH)	Enhances wettability and SEI formation	Improves Na^+ adsorption and electrolyte compatibility	Promotes K^+ binding and reversible redox reactions	Anchors Zn^{2+} ions; stabilizes aqueous electrolyte interface	Adds pseudocapacitance and improves wettability
Heteroatom doping (N, S, P, B)	Introduces defects and redox-active sites	N/S/P doping boosts Na^+ capacity and conductivity	N-doping enhances K^+ adsorption and rate performance	N-doping improves Zn^{2+} ORR activity; P/S enhance redox behavior	N/S/P doping adds pseudocapacitance and conductivity
Morphology (Fibrous, Aerogels, Nanosheets)	Buffers volume changes and shortens ion paths	CNC-based aerogels improve Na^+ cycling stability	Fibrous networks resist K^+-induced expansion	Nanofibers buffer Mg^{2+}/Zn^{2+} stress; improve mechanical stability	Aerogels offer ultralight, porous structures for high power
Composite formation (Carbon + Active Material)	Enhances conductivity and buffers stress	Carbon/metal sulfide hybrids improve Na^+ retention	Carbon/alloy composites stabilize K^+ cycling	Carbon/MnO_2 hybrids enhance Zn^{2+} capacity and stability	Carbon/polymer/ oxide hybrids boost capacitance and durability

For SIBs, we can identify that cellulose-derived carbons can be classified into several unique roles, as also compared in Table 2, (i) ion diffusion facilitators, where hierarchical porosity and tunable interlayer spacing enable efficient Na^+ transport; (ii) conductive matrices, in which graphitic domains and heteroatom doping (N, S, P, and B) improve electronic conductivity and create additional ion adsorption sites; (iii) surface stabilizers, where oxygen-rich groups enhance electrolyte wettability and help form a stable SEI layer; and (iv) structural buffers in composites, where cellulose-derived carbon frameworks combine with oxides, sulfides, or polymers to accommodate volume changes during cycling. This classification highlights how morphology control, surface chemistry, and hybrid integration distinctly contribute to improved electrochemical performance in SIBs.

5.2 | Potassium-Ion Batteries (KIBs)

The exploration of potassium-ion (K-ion) storage systems is gaining momentum due to their cost advantages over lithium-ion (Li-ion) counterparts, particularly in the context of graphite-based intercalation compounds. However, graphite's suboptimal performance, mainly due to significant volume expansion during K-ion intercalation, has prompted the search for alternative electrode materials. Among these, cellulose-derived carbons offer unique structural and chemical properties that address key challenges in KIBs, such as the large ionic radius of K^+ and potential structural degradation during cycling.

The most important advantage of cellulose-derived carbon in KIBs is its flexibility in designing the pore structure, which

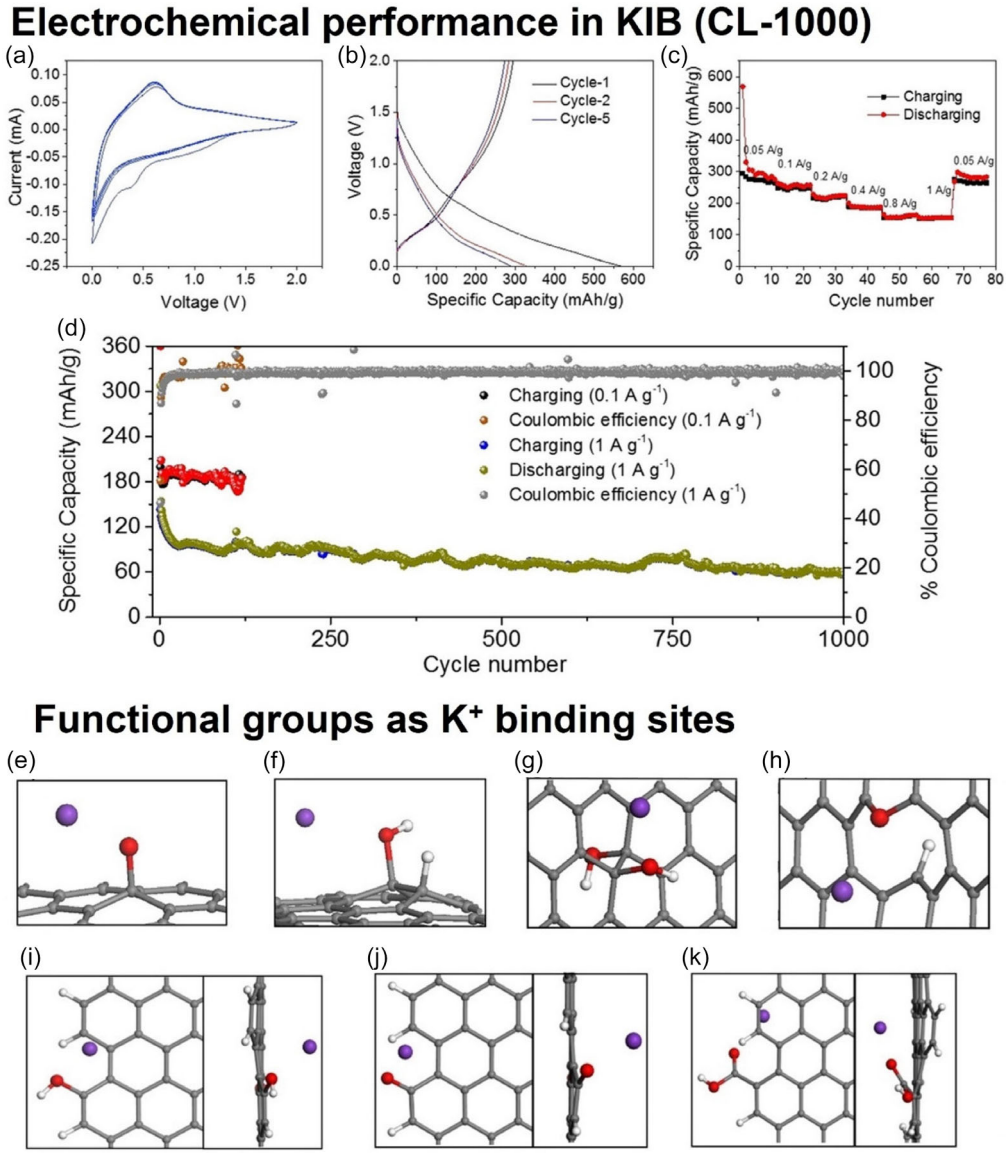

FIGURE 12 | Influence of functional group containing cellulose-derived carbon (CL-1000) pyrolyzed at 1000°C, on the KIB electrochemical performance, (a) cyclic voltammetry, (b) charge–discharge curve, (c) rate tolerance, (d) cycling stability, and schematic views of K binding sites of (e) epoxide (K–O: 2.35 Å), (f) hydroxyl (K–O: 2.62 Å), (g) double-sided hydroxyl (K–O: 2.56 Å), (h) O-doped graphene (K–O: 2.73 Å), and functional groups at the edge with side views: (i) hydroxyl of armchair graphene nanoribbon (AGNR), HO-AGNR (K–O: 2.80 Å), (j) O-AGNR (K–O: 2.44 Å), and (k) HOOC-AGNR (K–O: 2.59 Å), where the purple atoms are K, white are H, red are O, and grey are C. Copyright 2020, Wiley [143].

can allow adequate penetration of larger K^+ ions [143]. Optimizing cellulose-derived carbon can yield materials with increased mesoporosity by precisely modifying carbonization conditions and precursor treatment. In a significant advancement, we have demonstrated a simple, one-step pyrolysis process (1000–1400°C) to synthesize trubostratic hard carbon from commercially available cellulose for use in KIBs [143]. While higher temperature pyrolysis (1300–1400°C) improved graphitization (with a decreasing D/G ratio), it also reduced the surface area. The carbon produced at 1000°C showed better K-ion storage capabilities, due to an expanded interlayer spacing (≈0.4 nm) and a turbostratic structure rich in oxygen-containing functional groups. These structural features help enhance K-ion storage, resulting in high capacity, excellent rate capability, and long cycle life with minimal volume changes (Figure 12a–d).

Both experimental and theoretical studies support that oxygen functional groups on the carbon surface significantly enhance K-ion storage capacity. Mechanistically, the expanded interlayer spacing reduces steric hindrance, allowing ion insertion with minimal volume change, which helps maintain capacity over more than 1000 cycles at high current densities. Furthermore, as shown in Figure 12e–k, improved performance is also linked to strong K^+ binding with epoxide, hydroxyl, and carbonyl groups. DFT calculations reveal that binding energies range from −1.78 to −3.13 eV, all of which are stronger than the cohesive energy of bulk potassium (−0.93 eV). This prevents K clustering and ensures stable ion adsorption during extended cycling. Notably, we found that K^+ does not form KOH upon interaction with hydroxyl groups, unlike Na^+ in sodium-ion batteries, which allows fully reversible redox processes on the surface. Importantly, this study highlights the importance of balancing surface functional groups and turbostratic domains. As oxygen-containing functionalities increase capacitive contributions and wettability, excessive amounts, especially strongly binding species like -COOH, may cause partial irreversibility. Compared to lithium and sodium, a relatively low diffusion coefficient of potassium ions presents a challenge in KIBs. This can be mitigated by optimizing the surface chemistry of carbon, which features (OH and -COOH) functional groups, promoting strong adsorption and interaction of K^+ ions within the cellulose-derived carbon framework. These surface functional groups can also improve electrode wettability, thereby enhancing electrolyte/active material contact. Such interactions are crucial for achieving efficient charge transfer at the electrode–electrolyte interface, thereby improving capacity and rate performance in KIBs. Li et al. [144] reported a porous carbon nanofiber foam derived from BC for improving KIB performance. The carbon nanofiber foam electrode, characterized by a 3D porous structure, exhibits excellent rate capability and long-term cycling stability. It maintained a stable capacity of 158 $mAhg^{-1}$ after 2000 cycles at 1000 mAg^{-1} and 122 $mAhg^{-1}$ after 1000 cycles at 5000 mAg^{-1}. The high surface area, combined with the high conductivity of CNFs, offers abundant K-ion storage sites. Kinetics analysis confirmed both capacitive and diffusion-controlled charge storage, thus highlighting the potential of carbon nanofiber foam for sustainable energy storage.

Significant volume expansion during K^+ insertion specifically contributes to electrode degradation in KIBs. Carbon derived from cellulose acts as a flexible matrix that could buffer these expansions. Its structure, resembling natural fibers, is crucial for absorbing the mechanical strain caused by the repeated intercalation/deintercalation of the ions. The resilience of these carbon-based electrodes enhances the cycle life of the batteries, maintaining high capacity over many charge and discharge cycles. Moreover, the lightweight nature of carbon reduces overall electrode density, which benefits the construction of energy-dense yet lightweight battery systems. The structural tailoring of cellulose-derived carbon is also critical for mitigating mechanical stresses induced by the intercalation and deintercalation of K^+ ions, thereby enhancing the structural integrity and electrochemical stability. The ability to tune pore size also enhances faster ionic transport, which is crucial for maintaining stable battery operation at higher current densities. As illustrated in Figure 13, Ojeda et al. developed cost-effective carbon electrode materials from CNC, designed for K-ion energy storage [145]. Their synthesis incorporated both conventional annealing and an expedited, energy-efficient microwave-assisted carbonization technique. A 2-step, 4-min process utilizing $ZnCl_2$ activation yielded microwave-produced micro/mesoporous carbon characterized by a high specific surface area (SBET≈1800 m^2g^{-1}). When evaluated in symmetric supercapacitors using a 0.5 M K_2SO_4 aqueous electrolyte, these CNC-derived carbons demonstrated a reversible capacitance of ≈66 Fg^{-1} and maintained 83% of their initial capacitance after 10,000 cycles.

In a notable contribution to KIB anode development, Ma et al. [146] introduced nitrogen-doped carbon nanofibers derived from BC through pyrolysis, aiming to enhance long-term K-ion storage stability. The nitrogen-doped carbon nanofibers electrode retained a reversible specific capacity of 81 $mAhg^{-1}$ after 3000 cycles at 1 Ag^{-1}, showing a capacity retention of 71%. DFT calculations suggest that nitrogen doping enhances K-ion adsorption, thereby improving electrochemical performance. Additionally, nitrogen-doped carbon nanofibers exhibited low voltage plateaus during cycling and a high relative energy density, making them suitable for KIBs as anode materials. In another approach, BC nanofibers served as scaffolds for forming polypyrrole (PPy) composites, which, after carbonization, yielded a 3D porous carbon network [147]. After carbonization, a 3D porous carbon network with short-range ordered carbon is formed for KIBs. Nitrogen doping from PPy enhanced electrical conductivity and created active sites, thereby improving the anodic performance. The carbonized BC@PPy (C-BC@PPy) anode exhibited a capacity of 248 mA hg^{-1} after 100 cycles at 50 mAg^{-1} and retained 176 mA hg^{-1} after 2000 cycles at 500 mAg^{-1}. DFT calculations indicated capacity was driven by N-doped and defective carbon, as well as pseudocapacitance, setting the path for future BC composites for energy storage.

Expanding the scope of cellulose-derived carbon to potassium–sulfur batteries, Goswami et al. [148] introduced an eco-friendly and biodegradable carbonized BC, modified with banana fiber, as a free-standing and binder-free sulfur host for cathodes. The cell utilizes the catholyte K_2S_6 for fabrication due to its high sulfur loading and even distribution, but this process induces a potassium side reaction. To address this, carbonized BC is applied as an interlayer to reduce the polysulfide shuttle effect. The cell achieves specific capacities of 437, 354, and 193 $mAhg^{-1}$ at 0.2, 0.7, and 1.2 C, respectively, with excellent long-term cycling performance, retaining 78% of its capacity after 200 cycles at

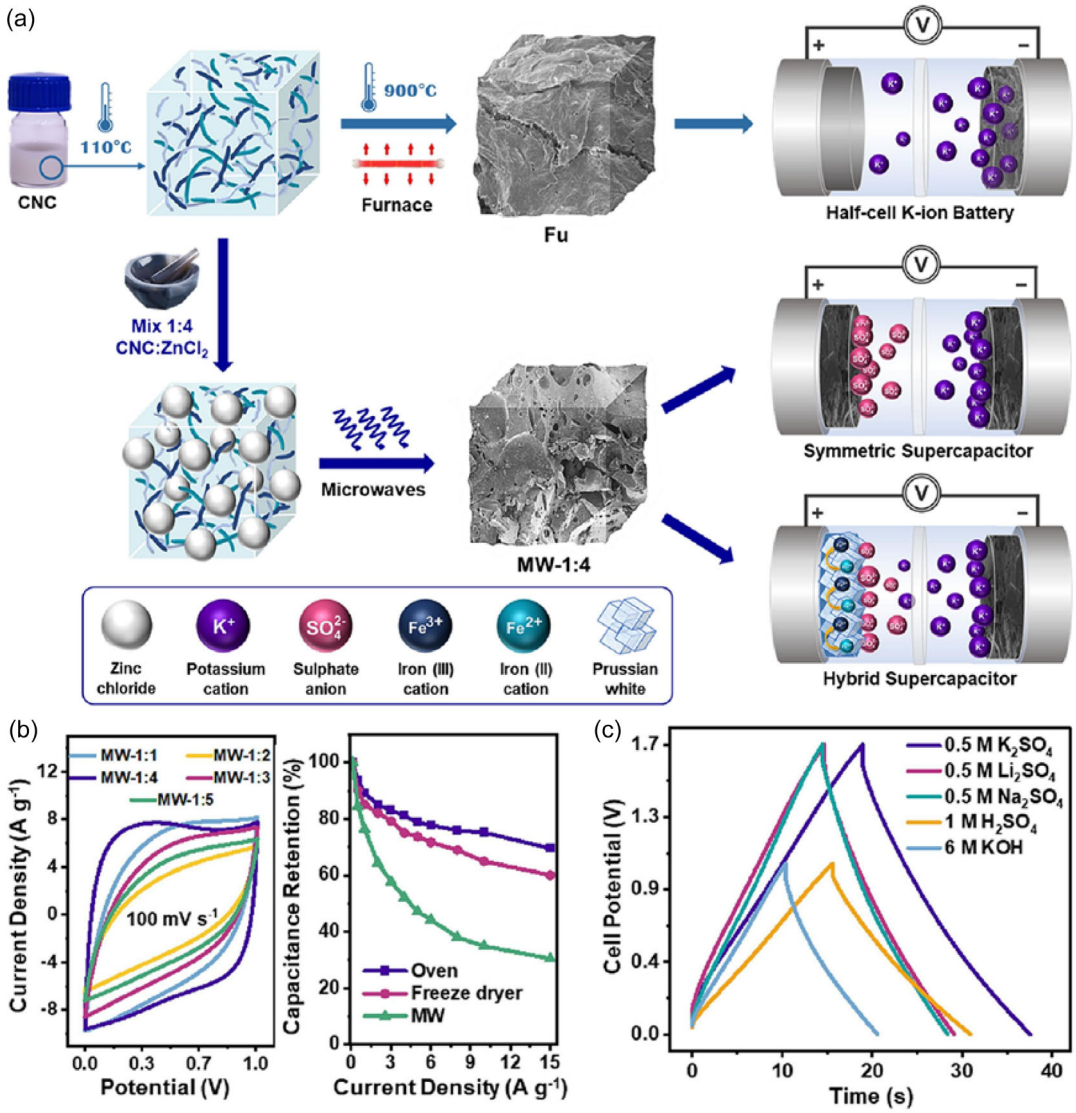

FIGURE 13 | (a) Illustration of the fabrication of nonactivated Fu and activated MW-1:4 samples and the various cell configurations utilized to evaluate the electrochemical characteristics of the carbon compounds generated from CNC. (b) The right side displays capacitance retention at different current densities for CNC-derived carbon electrodes synthesized with a CNC_2 ratio of 1:4 and various drying techniques before microwave (MW) synthesis. In contrast, the left side displays cyclic voltammograms (CVs) of carbon samples prepared with varying CNC_2 ratios (1:5 to 1:1) at a cycling rate of 100 mVs^{-1}. (c) The performance of CNC-derived porous carbon supercapacitors, made with an optimized CNC_2 ratio of 1:4, is evaluated at 5 Ag^{-1} in two-electrode symmetric cells using galvanostatic charge–discharge curves in aqueous electrolytes. Copyright 2024, Elsevier [145].

0.7 C. Thus, these works demonstrate a cost-effective and environmentally friendly method for creating high-performance potassium–sulfur batteries.

Another key research area for cellulose-derived carbon in KIBs is its integration with alloy-based active anode materials, such as Sn or Si, which undergo significant volume changes during charging and discharging. The carbon matrix helps buffer this expansion and forms a conductive network, enhancing the electrode's overall conductivity when combined with cellulose-derived carbon. This synergy contributes to more stable KIB performance. Such advancements facilitate the development of more durable and efficient energy storage systems, which are well-suited for large-scale applications. This includes vital sectors such as grid storage and electric vehicles, where KIBs are being intensively studied as a potentially cheaper alternative to traditional Li-ion batteries.

For KIBs, cellulose-derived carbons also play unique and classifiable roles: (i) accommodators of large K^+ ions, achieved through expanded interlayer spacing and turbostratic disorder that mitigate lattice strain; (ii) surface functional hosts, where oxygen-containing groups aid ion adsorption and maintain wettability; (iii) mechanical stabilizers, with fibrous carbon networks providing resilience against severe volume fluctuations; and (iv) conductivity enhancers in composites, particularly through nitrogen doping or coupling with alloy-type anodes, which improve electron transport and cycling stability.

Cellulose-derived carbons synthesized at moderate pyrolysis temperatures offer the most effective balance between expanded interlayer spacing, turbostratic disorder, and oxygen-rich surface functionalities, which collectively facilitate rapid and reversible K^+ storage with minimal structural degradation. These results

emphasize that controlling the interplay between turbostratic domains and specific oxygen groups (epoxide, hydroxyl, and carbonyl) is key to preventing irreversible reactions while maintaining long cycle stability in KIB anodes.

5.3 | Zinc-Ion Batteries (ZIBs)

In recent years, carbon derived from cellulose has been considered a promising electrode material for ZIBs, addressing some vital challenges associated with zinc-ion storage. One of the primary advantages of carbon is that it can serve as a host material to accommodate relatively large and divalent Zn^{2+} ions during charge and discharge cycles. The porous structure of cellulose-derived carbon provides a pathway for efficient ion diffusion, further reducing the kinetic sluggishness of Zn^{2+} migration within the electrode [149]. In particular, this porosity is especially beneficial in ensuring the uniform deposition of Zn^{2+} during cycling, preventing, for instance, dendrite formation in ZIBs, a potential cause for short circuits and capacity fade.

Another important feature of cellulose-derived carbon for use in ZIBs is its chemical stability in aqueous environments. Typically, ZIBs operate with aqueous electrolytes and often encounter issues such as electrode corrosion or passivation with conventional materials. However, the natural hydrophobicity and surface chemistry of cellulose-derived carbon, especially after carbonization and proper modification, further enhance its resistance to electrolyte-induced degradation. Carbon surface functional groups serve as sites for Zn^{2+} adsorption, enabling reversible zinc ion storage and improving capacity and cycling stability [149]. Another challenge in ZIBs is electrode stability during zinc ion insertion and extraction, which cellulose-derived carbon helps to address. The flexible, fiber-like nature of the cellulose carbon matrix provides excellent mechanical stability by helping to buffer the volume changes associated with zinc ion intercalation. This becomes important for preventing electrode cracking or delamination over repeated cycles [150]. This is a crucial factor for the commercial development of ZIBs, as the structural integrity of cellulose-derived carbon enables high reversibility and longer cycling life. Its lightweight structure decreases the overall electrode mass, making it beneficial for applications that require high energy density.

Beyond its role as an electrode material, cellulose-derived carbon exhibits excellent performance in composite systems combined with other active materials for zinc-related applications. For example, when paired with metal oxides such as MnO_2, it creates hybrid electrodes with enhanced electrochemical activity. In these composites, cellulose-derived carbon functions as a conductive backbone, facilitating electron transport and controlling the volume expansion of the metal oxide during zinc-ion cycling. The synergy between cellulose-derived carbon and active zinc species enhances capacity and cycling stability in ZIBs. This boost in rate performance makes them more suitable for applications such as grid energy storage or large-scale backup power. For instance, as shown in Figure 14, Liang developed a nitrogen-doped carbon nanofiber aerogel electrocatalyst for the oxygen reduction reaction (ORR) from BC. This aerogel features 5.8 at.% N-containing active sites and a 916 m^2g^{-1} BET surface area, and hence demonstrates a range of desirable ORR activity, selectivity, and stability in alkaline media [150]. The nitrogen-doped carbon nanofiber aerogel outperforms many metal-free catalysts. Its performance rivals that of Pt/C in Zn-air batteries, underlining its potential as a sustainable alternative to fuel cells and metal-air batteries.

Cellulose-derived carbon offers a porous, flexible, and chemically active framework that enables stable Zn^{2+} storage, prevents dendrite formation, buffers volume changes, and enhances electrochemical performance, making it a promising material for high-performance zinc-based batteries.

5.4 | Magnesium-Ion Batteries (MIBs)

Carbon derived from cellulose has emerged as a promising candidate for applications in MIBs, overcoming many issues associated with the divalent nature of Mg^{2+} ions. Among the key challenges in MIBs, poor Mg^{2+} diffusion in electrode materials cannot be overlooked, which is closely related to the high charge density and the relatively large ionic radius. The porous structure of cellulose-derived carbon, which can be tuned across a wide range, provides sufficient pathways for Mg^{2+} transport and storage, enabling fast ion diffusion. Consequently, it enhances the kinetics of magnesium insertion and extraction. Micro and mesopores within the hierarchical pore structure improve Mg^{2+} ion mobility, addressing one of the major hurdles in developing MIBs.

Electrode material selection in MIBs is crucial, as strong interactions between Mg^{2+} ions and the host matrix can cause sluggish ion intercalation. The surface properties of cellulose-derived carbon can be tailored to improve interaction with Mg^{2+} without significantly increasing the binding energy, enabling reversible magnesium storage. In this context, an effective carbonization and post-treatment activation process can preserve functional groups such as -OH and -COOH in cellulose-derived carbon, which facilitates Mg^{2+} adsorption and enhances charge storage capacity. Additionally, surface modification can enhance electrolyte compatibility, thereby stabilizing the electrode–electrolyte interface and ensuring good cycling performance in MIBs.

Recent studies have leveraged these advantages to develop high-performance MIB anodes. For example, Liu et al. synthesized CNCs within bimetallic Bi–Sn micro/nanospheres (CNC-CA@Bi-NS) (Figure 15), using ion-induced gelation and in situ thermal reduction, embedding CNC-CA@Bi-NS [151]. The electrode, used as an anode for MIBs, exhibited a high reversible specific capacity of 334 mAh/g after 100 cycles at 100 mAg^{-1}, with a superior rate performance and a long cycle life of 187 $mAhg^{-1}$. A capacity fade rate of 0.099% per cycle was achieved over 500 cycles at a current density of 1 Ag^{-1}. Specifically, carbon matrices enhance Mg^{2+} transport and buffer volume changes that enable this degree of performance. The dual-phase microstructure and the 3D nanoporous structure, along with carbon matrices, are deemed a promising strategy to achieve a biphasic Bi–Sn-combined 3D carbon aerogel. In another study, Cheng et al. [152], developed a unique CNC-derived carbon aerogel hybrid, with Bi nanosphere (4–9 nm) attached to the carbon matrix (CNC-CA@Bi-NS) to develop an anode for MIBs. Their approach utilized ion-induced gelation and in situ thermal reduction to

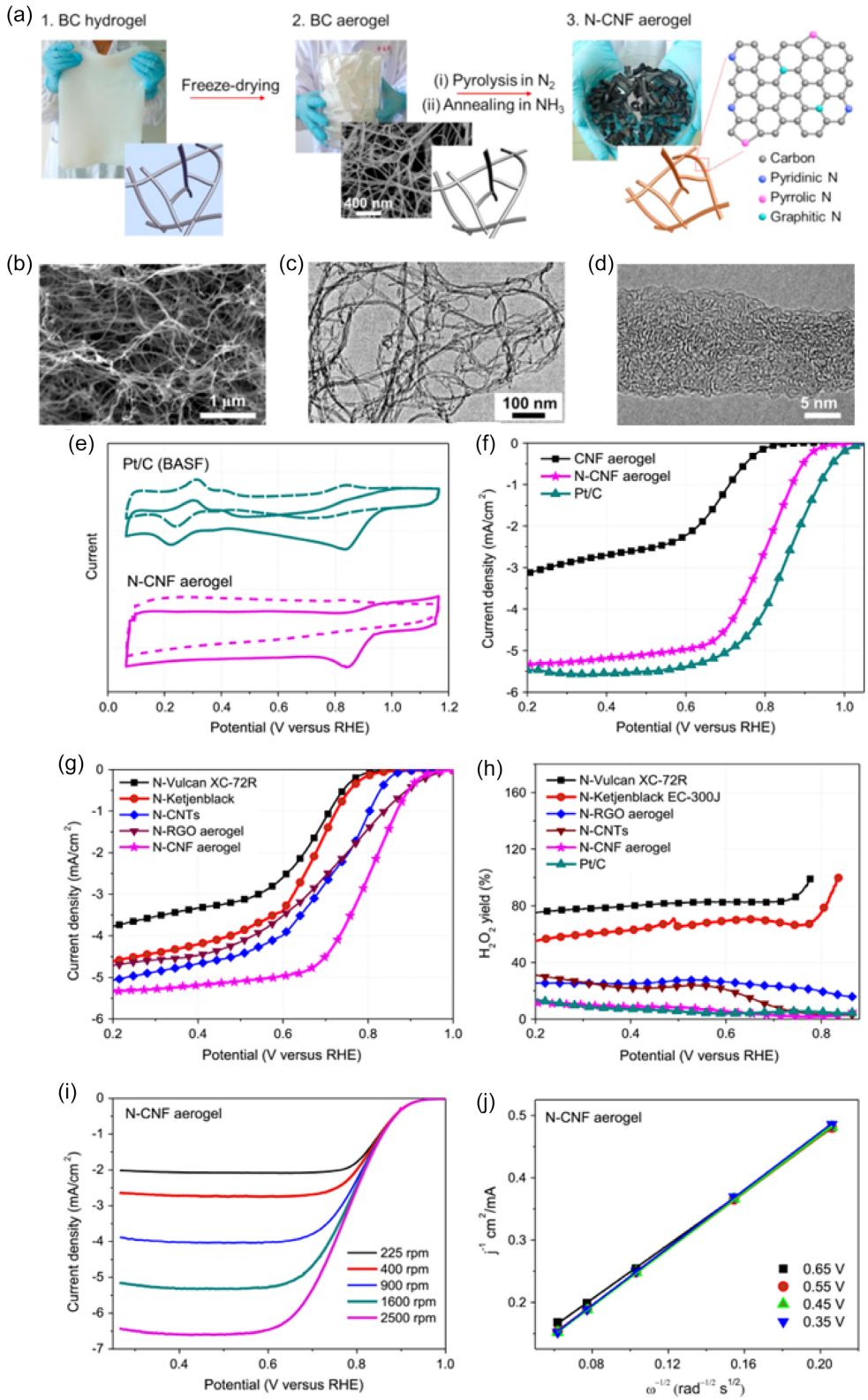

FIGURE 14 | Nitrogen-doped carbon nanofiber aerogels are illustrated. (a) Schematic illustration shows the process: (1) Large BC pellicles are produced via industrial microbial fermentation, (2) BC aerogels are formed by cutting and freeze-drying, and (3) black nitrogen-doped carbon nanofiber aerogels are obtained after heat treatments in N_2 and NH_3 atmospheres, with nitrogen-doped into the carbon matrix. (b,c) SEM and TEM images reveal the nanofibrous network of nitrogen-doped carbon nanofiber aerogels. (d) HR-TEM image shows a detailed structure of an individual nitrogen-doped carbon nanofiber. The ORR performance of reference catalysts and nitrogen-doped carbon nanofiber aerogels. (e) nitrogen-doped carbon nanofiber aerogels, along with Pt/C in O_2- and Ar-saturated KOH, are displayed in current–voltage curves. (f) Plots of ORR polarization contrast Pt/C, N-CNF aerogel, and carbon nanofiber aerogel. (g) The ORR performance of nitrogen-doped carbon nanofiber aerogel is contrasted with that of carbon materials treated with NH_3. (h) Plots of H_2O_2 yield for reference catalysts and nitrogen-doped carbon nanofiber aerogel. (i) N-CNF aerogel ORR polarization at varying velocities. (j) Koutecky–Levich (K–L) graphs demonstrate kinetic behavior during ORR at different potentials. Copyright 2015, Elsevier [150].

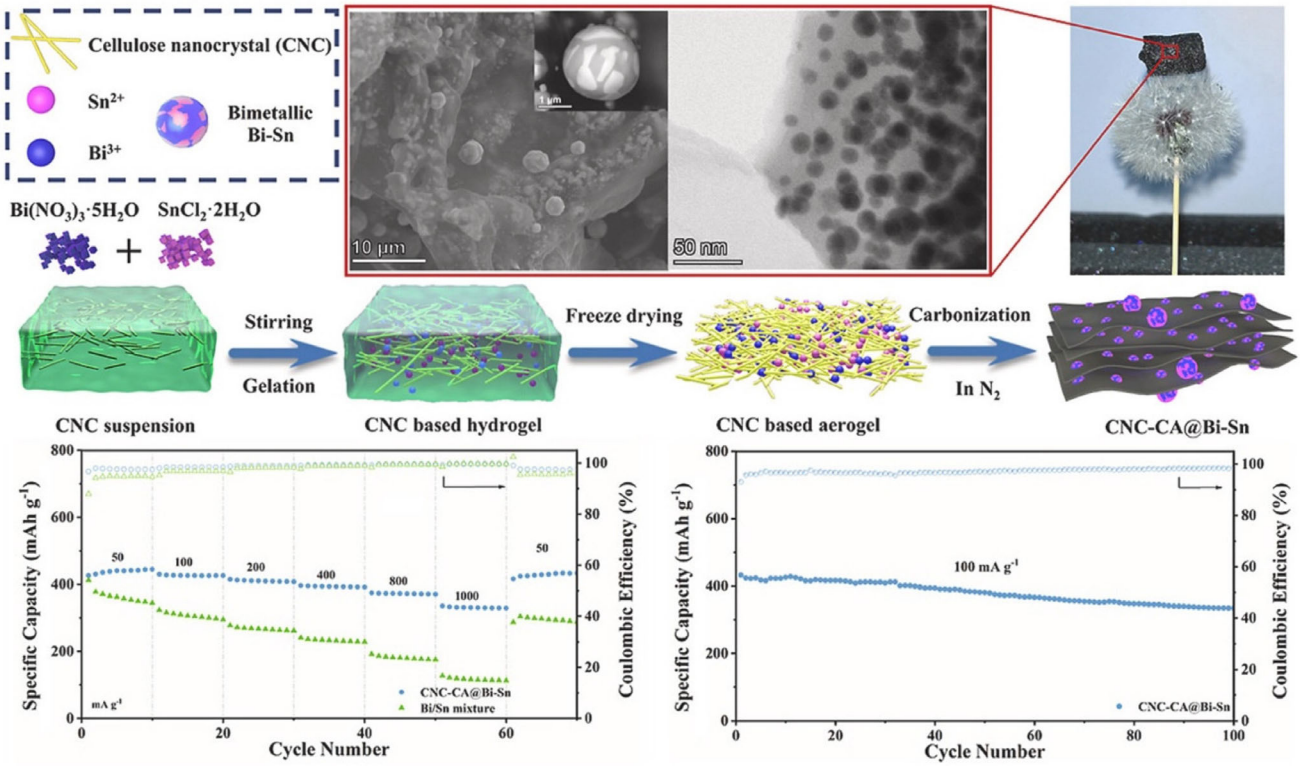

FIGURE 15 | A CNC suspension was solidified using $Bi(NO_3)_3{\cdot}5H_2O$ and $SnCl_2$, followed by freeze-drying and thermal reduction, to synthesize a lightweight, porous carbon aerogel with high specific capacity and Coulombic efficiency. Copyright 2023, Elsevier [151].

minimize volume changes and prevent agglomeration during magnetization. After 100 cycles, the CNC-CA@Bi-NS electrodes displayed a reversible specific capacity of 346 $mAhg^{-1}$. This signifies another promising approach to constructing high-performance MIB anodes with Bi-based materials, which exhibit nearly 100% coulombic efficiency after 5000 cycles at 2.0 C.

One of the key advantages of cellulose-derived carbon in MIBs is its structural stability, which allows it to withstand the mechanical stresses associated with magnesium intercalation. Unlike monovalent ions such as Li^+ or Na^+, the divalent Mg^{2+} ions exert considerable stress on electrode materials. The natural fibrous structure inherited from cellulose enables these types of carbon materials to absorb stresses, which helps prevent electrode degradation over multiple charge–discharge cycles and ensures long-term cycling stability for MIBs, without the volume changes and mechanical failure that often occur with other electrode materials. Moreover, cellulose-derived carbon has been utilized in composite structures for MIBs, where it serves as a conductive matrix to host magnesium-active materials, such as metal sulfides or oxides. In these hybrid systems, cellulose-derived carbon enhances overall electrode conductivity and mitigates the significant volume expansion commonly observed in magnesium-active materials during cycling. This combination has enhanced rate capability and capacity retention in MIBs, paving the way for more energy-dense and efficient magnesium-ion storage systems. Notably, cellulose-derived carbon leads the way in developing high-performance next-generation MIB technologies. Cellulose-derived carbon is a highly promising anode material for magnesium-ion batteries, offering hierarchical porosity for efficient Mg^{2+} diffusion, surface functional groups for reversible ion adsorption, and a fibrous structure that buffers mechanical stress. When used in composites with Mg-active materials, it enhances conductivity, mitigates volume expansion, and improves cycling stability and rate performance, making it ideal for high-performance, long-life MIBs.

5.5 | Supercapacitors and Emerging Energy Storage Systems

The tunable properties of cellulose-derived carbon make it a versatile candidate for supercapacitor as well [22]. To this end, carbon properties play a central role in advancing supercapacitor technologies, particularly hybrid systems that bridge the gap between batteries and traditional capacitors. The characteristics mentioned above, particularly the large surface area, enable rapid ion adsorption and desorption, which is a key criterion to achieve high power density [45]. Moreover, its chemical stability and structural flexibility enable integration with pseudocapacitive materials, such as transition metal oxides, to significantly enhance the charge storage capacity. Its surface chemistry is another crucial factor that affects performance. Depending on the temperature and atmosphere used, -OH/-COOH groups reside on the surface during the functionalization and carbonization process. These oxygen-containing groups enhance the wettability of the carbon surface, facilitating better electrolyte penetration and improved ion transport [44]. Additionally, these functional groups could contribute a Faradaic component to the overall capacitance as pseudocapacitance. Although most supercapacitors store charge through electrostatics, pseudocapacitance is another method for further improving energy storage capacity [153].

Our recent studies on sorghum-derived biocarbon have demonstrated how the structural and compositional diversity of lignocellulosic biomass directly governs the characteristics and electrochemical performance of the resultant carbon materials. By partitioning sorghum (Sugargraze) biomass into leaf, sheath, and stem sections, we identified distinct carbon morphologies linked to the varying lignin, cellulose, and ash contents of each component [44]. The leaf, rich in lignin and ash, produced carbon with higher crystallinity and graphite-like domains, whereas the sheath, with higher cellulose content, yielded thinner graphitic layers, larger interlayer spacing, and enhanced porosity. The bottom stem generated the highest carbon yield (30%) with more disordered, turbostratic structures, while the upper stem produced carbon of lower porosity and surface area. Complementary work using chemically refined sorghum biomass further clarified these relationships: cellulose-rich precursors, achieved through mild alkali or bleaching treatments, yielded carbons with superior surface area, pore volume, and capacitance values of up to 140 $F\,g^{-1}$ after activation, matching or surpassing those of commercial activated carbons. In contrast, lignin and hemicellulose were shown to impede electrochemical performance, despite aiding in graphitization [45]. Together, these studies reveal that careful biomass selection and compositional tuning of sorghum feedstocks can strategically tailor the porosity, graphitic order, and capacitance of biocarbons, also highlighting sorghum, like agricultural crop residues, as sustainable and tunable precursors for high-performance energy storage materials.

Recent studies have demonstrated that doping cellulose-derived carbon with heteroatoms, such as nitrogen, phosphorus, and sulfur, can further enhance electrochemical performance [154]. While nitrogen doping introduces defects in the carbon structure that act as active sites for ion adsorption, enhancing conductivity, sulfur and phosphorus create redox-active sites that contribute additional pseudocapacitance. Similarly, the introduction of sulfur and phosphorus dopants can create redox-active sites on the carbon surface, thereby contributing additional pseudocapacitance. These doping techniques enable the precise tailoring of cellulose-based carbons to meet specific performance goals, such as high energy density or fast charge–discharge cycles [155].

Furthermore, combining cellulose-derived carbon with other electrode materials can produce hybrid supercapacitors with superior performance. For example, composites of cellulose-derived carbon with metal oxides, such as MnO_2, or conducting polymers, such as PANI, have demonstrated improved specific capacitance and cycling stability in supercapacitors [156]. The carbon matrix serves as a conduction network, facilitating electron transport and absorbing volume changes associated with the redox reactions of metal oxides or polymers. In this hybrid system, the benefits of both materials are combined: the rapid ion transport of carbon and the high capacitance of the redox-active components result in supercapacitors with enhanced energy storage capacity and fast charge–discharge capabilities.

In aluminum-ion batteries (AIBs), the trivalent aluminum ion (Al^{3+}) presents challenges due to its large ionic radius and high charge density, which hinder ion diffusion and storage [157]. Cellulose-derived carbon offers a promising solution. The highly porous structure will facilitate efficient ion transport, enhancing rate performance. Additionally, the carbon matrix helps buffer volume changes during cycling, resulting in enhanced cycle life and improved overall battery stability [158].

In lithium–sulfur batteries, polysulfide dissolution is a major hurdle that leads to capacity fading and poor cycle life. The porous structure of cellulose-derived carbon can trap polysulfide intermediates, preventing them from dissolving into the electrolyte and thereby mitigating shuttle effects [159]. This can help extend the lifespan and improve overall efficiency. Additionally, the large surface area may provide abundant sites for sulfur deposition, enabling higher sulfur loading and, consequently, higher energy density. The enhanced electrical conductivity through the carbon matrix may lead to improved charge transfer and a more efficient use of the sulfur-active material.

Beyond energy storage, cellulose-derived carbon is being explored in capacitive deionization (CDI) for water desalination [160, 161]. In CDI, these carbons effectively adsorb ions for water desalination under an applied electric field, resulting in improved ion removal due to their hierarchical pore structures [162]. Hybrid devices that combine CDI with energy storage are also under investigation, offering the potential for simultaneous desalination and energy recovery.

Overall, the electrochemical performance of batteries and supercapacitors is closely governed by the interplay between porosity, degree of graphitization, interlayer spacing, and surface functionalities. As compared in Table 2, in SIBs, an expanded interlayer spacing and hierarchical porosity are crucial for accommodating the larger Na^+ ions, while heteroatom doping enhances electronic conductivity and reversible capacity. For KIBs, a moderate level of turbostratic disorder and oxygen-rich surfaces promote reversible K^+ adsorption and alleviate structural strain during cycling. In magnesium- and zinc-ion batteries, fibrous carbon morphologies with abundant surface functional groups buffer mechanical stress and facilitate stable ion transport, particularly in aqueous electrolytes. Meanwhile, supercapacitors rely on high specific surface area and optimised pore distribution to ensure rapid ion diffusion and efficient charge storage, often supported by pseudocapacitive effects from heteroatom doping. Hence, the tunable nature of cellulose-derived carbon makes it a promising and sustainable platform adaptable to diverse electrochemical systems. However, despite these advantages, challenges remain in achieving precise structural control, scalable production, and long-term stability under different ion chemistries. Addressing these limitations is critical, as described in the following section.

6 | Challenges and Future Works

A major challenge in producing cellulose-derived carbon for postlithium energy storage technologies is scalability. While diverse synthesis methodologies, including pyrolysis and HTC, are effective in producing high-quality carbon materials, significant concerns persist regarding their scalability for large-scale industrial deployment. Importantly, these production processes involve tightly controlled conditions that are typically

energy-intensive and time-consuming, such as slow pyrolysis and HTC. Future development must focus on designing more energy-efficient, cost-effective, and scalable methods to enable the widespread use of cellulose-derived carbon in energy storage [163]. This will require improving reactor design, optimizing process efficiency, and adopting continuous production methods. The refinement of structural and electrochemical properties of cellulose-derived carbon remains a key challenge. While such materials often have adjustable porosity, surface area, and conductivity, tailoring them for specific battery chemistries, such as SIBs or KIBs, is a complex process. For example, although high porosity can enhance ion transport and storage, excessive porosity may lead to structural instability and lower energy density. Additionally, carbonization often leaves the carbon surface rich in oxygen-containing functional groups, which can either positively or negatively influence the electrochemical performance. Future efforts should aim to optimize synthesis parameters, such as temperature and activation conditions, to better customize cellulose-derived carbon for enhanced performance in various post-lithium storage systems [160].

Another challenge is the compatibility of cellulose with various electrolytes and electrode configurations. In postlithium technologies, such as SIBs and ZIBs, the efficiency, durability, and safety of the battery largely depend on the behavior of the electrode/electrolyte interface [164]. Cellulose-derived carbon often lacks the necessary chemical stability or conductivity for specific electrolytes. Furthermore, the long-term cycle stability of these carbon materials should be evaluated, as their efficiency typically decreases during continuous charge and discharge cycles. Additionally, surface modification and doping techniques involving heteroatoms require further research to enhance electrolyte compatibility and achieve high cycling stability. Environmental and economic factors must also be considered for cellulose-derived carbon. Although these materials are inherently sustainable due to their biomass origin, it is crucial to carefully assess their carbon footprint, energy use, and waste management throughout the production process. Ultimately, utilizing low-cost and abundant biomass feedstocks while developing low-energy, waste-reducing synthesis methods will enhance the economic viability of cellulose-derived carbon for practical energy storage systems. The approach should incorporate green chemistry principles to improve the production process and ensure that carbon derived from cellulose remains a sustainable option for the future of postlithium energy storage.

7 | Conclusions

Cellulose-derived carbon holds significant promise for transforming energy storage beyond lithium-ion battery technology, due to its renewable source, versatile properties, and eco-friendly manufacturing. It can be implemented in new technologies, such as sodium, potassium, and zinc-ion-based batteries, as well as supercapacitors, where it has the potential to improve capacity, rate capability, and cycle stability. Various synthesis methods, such as pyrolysis, HTC, and activation, allow customization of shape, porosity, and surface chemistry to suit specific energy storage needs. Nonetheless, challenges remain in large-scale production, structural refinement, and long-term stability within different systems, despite their advantages. Future research should focus on scalable synthesis, lifecycle analysis, and integration with emerging chemistries, such as calcium-ion and dual-ion batteries. Overcoming these hurdles requires focused efforts on cost-effective and scalable methods, as well as an understanding of the electrochemical performance of carbon in postlithium contexts. As the industry moves toward sustainable high-performance materials, cellulose-derived carbon could lead the biochar movement, promoting greener and more efficient energy storage solutions.

Author Contributions

Vimukthi Dananjaya: data curation (equal), formal analysis (equal), visualization (equal), writing – original draft (equal), writing – review & editing (supporting). **Nethmi Hansika**: data curation (equal), formal analysis (equal), writing – original draft (equal). **Venkata Chevali**: formal analysis (supporting), visualization (supporting), writing – review & editing (equal). **Pratheep Kumar Annamalai**: conceptualization (equal), data curation (equal), formal analysis (equal), investigation (equal), project administration (equal), validation (equal), visualization (equal), writing – original draft (equal), writing – review & editing (equal). **Nisa Salim**: supervision (supporting), writing – review & editing (supporting). **Lei Ge**: visualization (supporting), writing – review & editing (supporting). **John Bell**: supervision (supporting), writing – review & editing (supporting). **Satyanarayanan Seshadri**: writing – review & editing (supporting). **Kothandaraman Ramanujam**: visualization (supporting), writing – review & editing (supporting). **Ashok Kumar Nanjundan**: conceptualization (equal), formal analysis (equal), funding acquisition (lead), project administration (lead), supervision (equal), validation (equal), visualization (equal), writing – original draft (equal), writing – review & editing (lead).

Acknowledgments

This work was funded by a capacity-building grant from the University of Southern Queensland. A.K.N. also acknowledges funding support from the Australian Research Council through the ARC Research Hub for Safe and Reliable Energy (IH200100035). P.K.A. acknowledges financial support from the SIMPLE Hub Regional Research Collaboration (RRC) Program grant from the Department of Education (Australian Government) and Queensland-Bavaria Research program grant (QLDBAVDEV20240040) from the Department of the Environment, Tourism, Science and Innovation (Queensland Government).

Open access publishing facilitated by University of Southern Queensland, as part of the Wiley - University of Southern Queensland agreement via the Council of Australian University Librarians.

Funding

This work was supported by University of Southern Queensland, Australian Research Council (IH200100035), Department of Education (Australian Government)- Regional Research Collaboration (RRC) Program (SIMPLEHub), and Department of the Environment, Tourism, Science and Innovation (Queensland-Bavaria Research Program) (QLDBAVDEV20240040).

Conflicts of Interest

The authors declare no conflicts of interest.

Data Availability Statement

The data that support the findings of this study are available from the corresponding author upon reasonable request.

References

1. T. Wilberforce, J. Thompson, and A. G. Olabi, Encyclopedia of Smart Materials 2 (2022), 1–7.

2. B. E. Lebrouhi, S. Baghi, B. Lamrani, E. Schall, and T. Kousksou, *Journal of Energy Storage* 55 (2022): 105471.

3. Y. S. Meng and M. E. Arroyo-de Dompablo, *Energy & Environmental Science* 2 (2009): 589–609.

4. R. Wanison, W. N. H. Syahputra, N. Kammuang-lue, et al., *Journal of Energy Storage* 100 (2024): 113497.

5. V. Balaram, M. Santosh, M. Satyanarayanan, N. Srinivas, and H. Gupta, *Geoscience Frontiers* 15 (2024): 101868.

6. H. Au, M. Crespo-Ribadeneyra, and M.-M. Titirici, *One Earth* 5 (2022): 207–211.

7. Y. Wang, R. Chen, T. Chen, et al., *Energy Storage Materials* 4 (2016): 103–129.

8. E. K. Savvidou, A. Rensmo, J. P. Benskin, et al., *Environmental Science & Technology* 58 (2024): 21908–21917.

9. J.-M. Tarascon, *Joule* 4 (2020): 1616–1620.

10. M. Kim, J. F. S. Fernando, J. Wang, et al., *Chemical Communications* 58 (2022): 863–866.

11. M. Xiao, X. Dai, and Y. Jiang, *Journal of Energy Storage* 111 (2025): 115411.

12. W. u. Rehman, Y. Ma, Z. khan, et al., *Next Materials* 7 (2025): 100450.

13. J. Wang, P. Nie, B. Ding, et al., *Journal of Materials Chemistry A* 5 (2017): 2411–2428.

14. M. Zhang, J. Zhang, S. Ran, W. Sun, and Z. Zhu, *Electrochemistry Communications* 138 (2022): 107283.

15. T. Khandaker, T. Islam, A. Nandi, et al., *Sustainable Energy & Fuels* 9 (2025): 693–723.

16. J. Wang, J. Gao, J. Zhang, et al., *Batteries & Supercaps* 5 (2022): e202100260.

17. K. Yu, J. Wang, K. Song, X. Wang, C. Liang, and Y. Dou, *Nanomaterials* 9 (2019): 93.

18. V. K. Bharti, A. P. Goswami, C. S. Sharma, and M. Khandelwal, *Journal of Electroanalytical Chemistry* 957 (2024): 118142.

19. F. Duffner, N. Kronemeyer, J. Tübke, J. Leker, M. Winter, and R. Schmuch, *Nature Energy* 6 (2021): 123–134.

20. E. Lizundia, C. M. Costa, R. Alves, and S. Lanceros-Méndez, *Carbohydrate Polymer Technologies and Applications* 1 (2020): 100001.

21. J. M. Zhang, Q. Hua, J. Li, et al., *ACS Omega* 3 (2018): 14933–14941.

22. C. Liu, H. Wang, X. Zhao, et al., *Journal of Power Sources* 457 (2020): 228056.

23. C. Yuan, H. Xu, S. A. El-khodary, et al., *Fuel* 362 (2024): 130795.

24. S. M. Ji and A. Kumar, *Polymers* 14 (2022): 169.

25. A. Siddiqa, Z. Yhobu, D. H. Nagaraju, et al., *Energy & Fuels* 37 (2023): 2498–2519.

26. H. He, R. Zhang, P. Zhang, et al., *Advanced Science* 10 (2023): 2205557.

27. H. Seddiqi, E. Oliaei, H. Honarkar, et al., *Cellulose* 28 (2021): 1893–1931.

28. T. Aziz, A. Farid, F. Haq, et al., *Polymers* 14 (2022): 3206.

29. M. M. Rana and H. De la Hoz Siegler, *Journal of Materials Research* 38 (2023): 328–336.

30. E. C. Emenike, K. O. Iwuozor, O. D. Saliu, J. Ramontja, and A. G. Adeniyi, *Carbohydrate Polymer Technologies and Applications* 6 (2023): 100337.

31. J. Verma, M. Petru, and S. Goel, *Industrial Crops and Products* 210 (2024): 118078.

32. N. A. Zainul Armir, A. Zulkifli, S. Gunaseelan, et al., *Polymers* 13 (2021): 3586.

33. Z. Ilham, in Value-Chain of Biofuels, ed. S. Yusup and N. A. Rashidi (Elsevier, 2022), 69–87.

34. M. Antlauf, N. Boulanger, L. Berglund, K. Oksman, and O. Andersson, *Biomacromolecules* 22 (2021): 3800–3809.

35. R. K. Pal, P. Goyal, and S. Sehgal, *Materials Today: Proceedings* 45 (2021): 5778–5781.

36. S. P. Kulkarni, *Biomass and Bioenergy* 184 (2024): 107182.

37. V. K. Gupta Suhas, P. J. Carrott, R. Singh, M. Chaudhary, and S. Kushwaha, *Bioresource Technology* 216 (2016): 1066–1076.

38. A. G. Dumanlı and A. H. Windle, *Journal of Materials Science* 47 (2012): 4236–4250.

39. A. E. Lewandowska, C. Soutis, L. Savage, and S. J. Eichhorn, *Composites Science and Technology* 116 (2015): 50–57.

40. K. S. Femina and A. Asokan, in Handbook of Biomass, ed. S. Thomas, M. Hosur, D. Pasquini, and C. Jose Chirayil (Springer Nature Singapore, 2023), 1–28, Ch. Chapter 20-1.

41. A. Winter, B. Arminger, S. Veigel, et al., *Cellulose* 27 (2020): 9325–9336.

42. M. Mujtaba, L. Fernandes Fraceto, M. Fazeli, et al., *Journal of Cleaner Production* 402 (2023): 136815.

43. P. González-García, *Renewable and Sustainable Energy Reviews* 82 (2018): 1393–1414.

44. J. Deng, T. Xiong, H. Wang, A. Zheng, and Y. Wang, *ACS Sustainable Chemistry and Engineering* 4 (2016): 3750–3756.

45. R. A. Afzal, J. Pennells, Y. Yamauchi, P. K. Annamalai, A. K. Nanjundan, and D. J. Martin, *Carbon Trends* 7 (2022): 100168.

46. R. A. Afzal, P. K. Annamalai, M. Tebyetekerwa, et al., *RSC Sustainability* 3 (2025): 1691–1704.

47. P. K. Annamalai, A. K. Nanjundan, D. P. Dubal, and J. B. Baek, *Advanced Materials Technologies* 6 (2021): 2001164.

48. S. Sayadi and F. Brouillette, *Carbohydrate Polymers* 343 (2024): 122500.

49. M. Stepanova and E. Korzhikova-Vlakh, *Polymers* 14 (2022): 1477.

50. M. Abdelmouleh, S. Boufi, M. N. Belgacem, A. P. Duarte, A. Ben Salah, and A. Gandini, *International Journal of Adhesion & Adhesives* 24 (2004): 43–54.

51. B. L. Holt, S. D. Stoyanov, E. Pelan, and V. N. Paunov, *Journal of Materials Chemistry* 20 (2010): 10058–10070.

52. T. Saito, R. Kuramae, J. Wohlert, L. A. Berglund, and A. Isogai, *Biomacromolecules* 14 (2013): 248–253.

53. M. Mariano, N. El Kissi, and A. Dufresne, *Journal of Polymer Science Part B: Polymer Physics* 52 (2014): 791–806.

54. A. Babaei-Ghazvini and B. Acharya, *Carbohydrate Polymer Technologies and Applications* 5 (2023): 100311.

55. R. Bacon and M. M. Tang, *Carbon* 2 (1964): 221–225.

56. Y. Shen, P. Wang, and L. Chen, *Fuel* 324 (2022): 124502.

57. M. M. Tang and R. Bacon, *Carbon* 2 (1964): 211–220.

58. G. Zhang, C. Chen, C. Xu, et al., *Energy and Fuels* 38 (2024): 8326–8336.

59. D. Chen, K. Cen, X. Zhuang, et al., *Combustion and Flame* 242 (2022): 112142.

60. M. R. Barr, M. Volpe, A. Messineo, and R. Volpe, *Fuel* 276 (2020): 118069.

61. J. Zhang, Y. S. Choi, C. G. Yoo, T. H. Kim, R. C. Brown, and B. H. Shanks, *ACS Sustainable Chemistry and Engineering* 3 (2015): 293–301.

62. J. Zhang, Y. An, A. Borrion, et al., *Bioresource Technology* 259 (2018): 91–98.

63. M. Sevilla and A. B. Fuertes, *Carbon* 47 (2009): 2281–2289.

64. V. Simone, A. Boulineau, A. de Geyer, D. Rouchon, L. Simonin, and S. Martinet, *Journal of Energy Chemistry* 25 (2016): 761–768.

65. C. E. Efika, J. A. Onwudili, and P. T. Williams, *Waste Management* 76 (2018): 497–506.

66. C. Bommier, R. Xu, W. Wang, et al., *Nano Energy* 13 (2015): 709–717.

67. J. L. Santos, M. A. Centeno, and J. A. Odriozola, *Journal of Analytical and Applied Pyrolysis* 148 (2020): 104821.

68. Y. Shao, C. Guizani, P. Grosseau, D. Chaussy, and D. Beneventi, *Carbon* 129 (2018): 357–366.

69. R. K. Mishra, M. Misra, and A. K. Mohanty, *ACS Omega* 7 (2022): 1612–1627.

70. R. Kumar Mishra, B. Singh, and B. Acharya, *Carbon Resources Conversion* 7 (2024): 100228.

71. X.-n. Ye, Q. Lu, X. Wang, et al., *ACS Sustainable Chemistry & Engineering* 5 (2017): 10815–10825.

72. A. Maaoui, A. Ben Hassen Trabelsi, A. Ben Abdallah, et al., *Journal of the Energy Institute* 108 (2023): 101242.

73. M. Carrier, M. Windt, B. Ziegler, et al., *ChemSusChem* 10 (2017): 3212–3224.

74. M. Pahnila, A. Koskela, P. Sulasalmi, and T. Fabritius, *Energies* 16 (2023): 6936.

75. K. H. Adolfsson, N. Yadav, and M. Hakkarainen, *Current Opinion in Green and Sustainable Chemistry* 23 (2020): 18–24.

76. K. Sheng, S. Zhang, J. Liu, et al., *Journal of Cleaner Production* 237 (2019): 117831.

77. D. Kim, K. Yoshikawa, and K. Park, *Energies* 8 (2015): 14040–14048.

78. M. Volpe, A. Messineo, M. Mäkelä, et al., *Fuel Processing Technology* 206 (2020): 106456.

79. C. Liu, K. Wang, Y. Du, Y. Shan, P. Duan, and N. Ramzan, *Polymers* 15 (2023): 4478.

80. I. Neme, G. Gonfa, and C. Masi, *Heliyon* 8 (2022): e11940.

81. D. Bosch, J. O. Back, D. Gurtner, S. Giberti, A. Hofmann, and A. Bockreis, *Carbon Resources Conversion* 5 (2022): 299–309.

82. I. J. Siddique, A. A. Salema, E. Antunes, and R. Vinu, *Renewable and Sustainable Energy Reviews* 153 (2022): 111767.

83. T. Qiu, C. Li, W. Zhao, M. Y. Naz, and Y. Zhang, *Biomass and Bioenergy* 193 (2025): 107583.

84. S. M. Selvam and B. Paramasivan, *Chemosphere* 286 (2022): 131631.

85. M. C. Holliday, D. R. Parsons, and S. H. Zein, *Processes* 10 (2022): 1756.

86. Y. Liu, C. Zhou, A. A. Siyal, et al., *Journal of Cleaner Production* 437 (2024): 140750.

87. X. Zhang, G. He, H. Sun, et al., *International Journal of Electrochemical Science* 19 (2024): 100617.

88. J. Quílez-Bermejo, E. Morallón, D. Cazorla-Amorós, A. Celzard, and V. Fierro, *Carbon* 237 (2025): 120151.

89. K. Kong, L. Deng, I. A. Kinloch, R. J. Young, and S. J. Eichhorn, *Journal of Materials Science* 47 (2012): 5402–5410.

90. A. Cuesta, P. Dhamelincourt, J. Laureyns, A. Martínez-Alonso, and J. M. D. Tascón, *Journal of Materials Chemistry* 8 (1998): 2875–2879.

91. E. Jiang, M. Maghe, N. Zohdi, et al., *ACS Omega* 4 (2019): 9720–9730.

92. L. Wannasen, N. Chanlek, W. Mongkolthanaruk, S. Daengsakul, and S. Pinitsoontorn, *Materials Science for Energy Technologies* 8 (2025): 13–23.

93. J.-S. Jeong, H.-M. Lee, and B.-J. Kim, *Energy Reports* 12 (2024): 2321–2327.

94. J. Gelfond, T. Meng, S. Li, T. Li, and L. Hu, *Sustainable Materials and Technologies* 35 (2023): e00573.

95. M.-L. Wang, S. Zhang, Z.-H. Zhou, et al., *Composites Part B: Engineering* 224 (2021): 109175.

96. M. Li, Y. Jia, L. Che, et al., *Thermochimica Acta* 751 (2025): 180061.

97. M. Liu, R. Chu, G. Li, et al., *Nano Energy* 138 (2025): 110852.

98. Y. Tong, F. Xue, X. Lu, et al., *International Journal of Biological Macromolecules* 320 (2025): 145681.

99. J. M. Spörl, R. Beyer, F. Abels, et al., *Macromolecular Materials and Engineering* 302 (2017): 1700195.

100. M. P. Vocht, A. Ota, E. Frank, F. Hermanutz, and M. R. Buchmeiser, *Industrial & Engineering Chemistry Research* 61 (2022): 5191–5201.

101. G. Guan, J. Li, X. Li, J. Xiang, and Y. Zhou, *Journal of Materiomics* 11 (2025): 100881.

102. M. Fan, C. Li, Y. Sun, L. Zhang, S. Zhang, and X. Hu, *Science of the Total Environment* 799 (2021): 149354.

103. Y.-R. Rhim, Z. Dajie, D. Nagle, M. Rooney, and C. Herman, in *ASME/JSME 2007 Thermal Engineering Heat Transfer Energy Conference*, Vol. 1 (2007), 911.

104. C. Pflieger, T. Eckhard, G. Schmitz, et al., *ACS Omega* 7 (2022): 48606–48614.

105. C. Wang, X. Wang, H. Lu, H. Li, and X. S. Zhao, *Carbon* 140 (2018): 139–147.

106. N. Sriplai and S. Pinitsoontorn, *Carbohydrate Polymers* 254 (2021): 117228.

107. Z. Wu, Z. Meng, C. Yao, Y. Deng, G. Zhang, and Y. Wang, *Materials Chemistry and Physics* 275 (2022): 125246.

108. Y. Li, L. Liu, W. Huang, et al., *Journal of Renewable Materials* 11 (2023): 3001–3023.

109. J. Li, T. Yuan, W. Zhu, et al., *Materials Today Communications* 41 (2024): 111029.

110. Y.-J. Tan, J. Li, Y. Gao, J. Li, S. Guo, and M. Wang, *Applied Surface Science* 458 (2018): 236–244.

111. J. Chen, Z. Zhu, H. Zhang, S. Tian, and S. Fu, *Materials & Design* 204 (2021): 109695.

112. V. Kuzmenko, A. M. Saleem, A. Bhaskar, H. Staaf, V. Desmaris, and P. Enoksson, *Journal of Physics: Conference Series* 660 (2015): 012062.

113. E. Jayamani, M. R. Rahman, and M. K. B. Bakri, in *Fundamentals and Recent Advances in Nanocomposites Based on Polymers and Nanocellulose*, ed. M. R. Rahman (Elsevier, 2022), 189–206.

114. L. Qin, S. Xu, Z. Lu, et al., *Diamond and Related Materials* 136 (2023): 110065.

115. P. Bishnoi, S. S. Siwal, V. Kumar, and V. K. Thakur, *Electron* 2 (2024): e42.

116. P. C. Ani, P. U. Nzereogu, A. C. Agbogu, F. I. Ezema, and A. C. Nwanya, *Applied Surface Science Advances* 11 (2022): 100298.

117. D. Xu, C. Chen, J. Xie, et al., *Advanced Energy Materials* 6 (2016): 1501929.

118. H. Jia, N. Sun, M. Dirican, et al., *ACS Applied Materials & Interfaces* 10 (2018): 44368–44375.

119. L. Shi, Y. Li, F. Zeng, et al., *Chemical Engineering Journal* 356 (2019): 107–116.

120. W. Luo, F. Shen, C. Bommier, H. Zhu, X. Ji, and L. Hu, *Accounts of Chemical Research* 49 (2016): 231–240.

121. B. Zhao, X. Li, L. Shang, et al., *Journal of Materials Chemistry A* 12 (2024): 5834–5845.

122. W. Luo, J. Schardt, C. Bommier, et al., *Journal of Materials Chemistry A* 1 (2013): 10662–10666.

123. R. R. Gaddam, D. Yang, R. Narayan, K. Raju, N. A. Kumar, and X. S. Zhao, *Nano Energy* 26 (2016): 346–352.

124. B. T. S. Ramanujam, A. K. Nanjundan, and P. K. Annamalai, Nanocellulose Based Composites for Electronics (2021), 295–312.

125. N. Amiralian, P. K. Annamalai, C. J. Garvey, E. Jiang, P. Memmott, and D. J. Martin, *Cellulose* 24 (2017): 3753–3766.

126. R. R. Gaddam, E. Jiang, N. Amiralian, et al., *Sustainable Energy & Fuels* 1 (2017): 1090–1097.

127. T. Chen, Y. Liu, L. Pan, et al., *Journal of Materials Chemistry A* 2 (2014): 4117–4121.

128. S.-J. Jiang, Y.-S. Xu, X.-W. Sun, et al., *Journal of the American Chemical Society* 147 (2025): 8088–8092.

129. M. Kim, J. F. S. Fernando, Z. Li, et al., *Chemical Engineering Journal* 445 (2022): 136344.

130. M. Kim, L. Ma, Z. Li, et al., *Journal of Materials Chemistry A* 11 (2023): 16626–16635.

131. Y. E. Kim, S. J. Yeom, J.-E. Lee, et al., *Journal of Power Sources* 468 (2020): 228371.

132. C. Yang, J. Xiong, X. Ou, et al., *Materials Today Energy* 8 (2018): 37–44.

133. Q. Jin, W. Li, K. Wang, et al., *Journal of Materials Chemistry A* 7 (2019): 10239–10245.

134. H.-m. Wang, H.-x. Wang, Y. Chen, et al., *Applied Surface Science* 273 (2013): 302–309.

135. H. Tao, L. Xiong, S. Du, Y. Zhang, X. Yang, and L. Zhang, *Carbon* 122 (2017): 54–63.

136. A. K. Thakur, K. Kurtyka, M. Majumder, et al., *Advanced Materials Interfaces* 9 (2022): 2101964.

137. Q. Shi, D. Liu, Y. Wang, Y. Zhao, X. Yang, and J. Huang, *Small* 15 (2019): e1901724.

138. L. Li, Q. Wang, X. Zhang, L. Fang, X. Li, and W. Zhang, *Applied Surface Science* 508 (2020): 145295.

139. X. X. He, J. H. Zhao, W. H. Lai, et al., *ACS Applied Materials & Interfaces* 13 (2021): 44358–44368.

140. F. Wang, X. Shi, J. Zhang, et al., *Nanoscale* 14 (2022): 3609–3617.

141. J. Wang, Z. Xu, J. C. Eloi, M. M. Titirici, and S. J. Eichhorn, *Advanced Functional Materials* 32 (2022): 2110862.

142. X. Chen, D. Zhao, X. Liu, Z. Gao, G. Wang, and X. Cao, *Materials Today Energy* 51 (2025): 101895.

143. A. K. Nanjundan, R. R. Gaddam, A. H. Farokh Niaei, et al., *Batteries & Supercaps* 3 (2020): 953–960.

144. H. Li, Z. Cheng, Q. Zhang, et al., *Nano Letters* 18 (2018): 7407–7413.

145. I. Ojeda, C. B. Arenas, R. Calle-Gil, et al., *Sustainable Materials and Technologies* 40 (2024): e00932.

146. L. Ma, J. Li, Z. Li, Y. Ji, W. Mai, and H. Wang, *Nanomaterials* 11 (2021): 1130.

147. Z. Liu, L. Yue, C. Wang, et al., *ACS Applied Materials & Interfaces* 15 (2023): 14865–14873.

148. A. P. Goswami, V. K. Bharti, C. S. Sharma, and M. Khandelwal, *Carbon Trends* 16 (2024): 100391.

149. L. Cheng, Y. Huang, S. Yin, et al., *Carbohydrate Polymers* 316 (2023): 121075.

150. H.-W. Liang, Z.-Y. Wu, L.-F. Chen, C. Li, and S.-H. Yu, *Nano Energy* 11 (2015): 366–376.

151. J. Liu, M. Cheng, Q. Liu, et al., *Composites Communications* 39 (2023): 101553.

152. M. Cheng, J. Liu, X. Wang, et al., *Chemical Engineering Journal* 451 (2023): 138824.

153. Y. Liu, S. P. Jiang, and Z. Shao, *Materials Today Advances* 7 (2020): 100072.

154. H. Lu, X. Sun, R. R. Gaddam, N. A. Kumar, and X. S. Zhao, *Journal of Power Sources* 360 (2017): 634–641.

155. R. Si, H. Luo, and J. Pu, *Industrial Crops and Products* 200 (2023): 116844.

156. S. A. Jadhav, S. D. Dhas, K. T. Patil, A. V. Moholkar, and P. S. Patil, *Chemical Physics Letters* 778 (2021): 138764.

157. G. S. D. Reis, S. Petnikota, C. M. Subramaniyam, et al., *Nanomaterials* 13 (2023): 765.

158. W.-L. Song, S. Li, G. Zhang, J. Tu, H.-S. Chen, and S. Jiao, *Sustainable Energy & Fuels* 3 (2019): 3561–3568.

159. Z. Zhang, Z. Fang, Y. Xiang, et al., *Carbohydrate Polymers* 255 (2021): 117469.

160. C. Zhang, D. Wang, Y. Qiu, et al., *Chemical Engineering Journal* 471 (2023): 144526.

161. X. Sheng, X. Xu, Y. Wu, et al., *Bulletin of the Chemical Society of Japan* 94 (2021): 1645–1650.

162. N. Pugazhenthiran, S. Sen Gupta, A. Prabhath, et al., *ACS Applied Materials & Interfaces* 7 (2015): 20156–20163.

163. F. Wang, T. Zhang, T. Zhang, T. He, and F. Ran, *Nano-Micro Letters* 16 (2024): 148.

164. J. Fischer, B. Pohle, E. Dmitrieva, K. Thümmler, S. Fischer, and D. Mikhailova, *Journal of Energy Storage* 55 (2022): 105725.

Biographies

Vimukthi Dananjaya is a Ph.D. researcher in the School of Engineering at Swinburne University of Technology, Australia. He obtained his bachelor's degree in applied sciences (Polymer Science and Technology) from the University of Sri Jayewardenepura, Sri Lanka. His research focuses on advanced materials and surface engineering for space applications, particularly the design of polymer coatings for passive lunar dust mitigation. His broader interests include nanocomposites, additive manufacturing, biodegradable polymers, and sustainable materials for aerospace and energy applications.

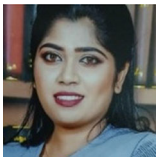

Nethmi Hansika is a researcher in the Department of Computer Engineering, Faculty of Engineering at the Open University of Sri Lanka. Her research interests include energy storage, sensors, computing, machine learning, and advanced technologies. She has contributed to several interdisciplinary studies exploring the integration of intelligent systems in energy and materials research. Nethmi develops innovative computational and data-driven approaches to address sustainability and efficiency challenges in modern engineering applications.

Venkata Chevali is an adjunct associate professor at the University of Southern Queensland. Integrating macromolecular chemistry and chemical engineering, his research focuses on accelerating the production of thermoplastic, fire-retardant, and sustainable polymer composites. He has collaborated extensively with industry to scale and commercialise composite technologies. Dr. Chevali has been a chief investigator on several major ARC projects, including a Discovery Project, a Linkage Infrastructure initiative, and the SIMPLE Hub for sustainable manufacturing. His international collaborations include leading experts from the University of Tennessee, Leibniz University, and Clemson University.

Pratheep Kumar Annamalai is a polymer and materials scientist and colead of the Medical Materials Technologies (SIMPLE Hub) team at the University of Southern Queensland (UniSQ), Australia. Earlier, he received his Ph.D. in Chemistry from Savitribai Phule Pune University, India. His current research focuses on renewable and recyclable polymers for biomedical, electronics, and industrial applications, supported by the Regional Research Collaboration and Queensland-Bavaria research programs funded by federal and state governments.

Nisa Salim is the director of Swinburne-CSIRO National Industry 4.0 Testlab for the automated composites manufacturing facility at Swinburne University of Technology, Australia. She received her Ph.D. degree from Deakin University with a highly prestigious gold medal for research excellence from the Australian Institute of Nuclear Science and Engineering. Her research team focuses on interdisciplinary science and engineering, including advanced composites manufacturing, materials science, and chemistry, enabling key applications in space, aerospace, and defence.

Lei Ge is an Australian research council future fellow and associate professor in the School of Engineering at the University of Southern Queensland, and an honorary associate professor in the School of Chemical Engineering at the University of Queensland, Australia. He completed his Ph.D. in 2013 at the University of Queensland. His research focuses on material development and process design for electrocatalysis, thermal catalysis, membrane gas separation and adsorption.

John Bell is deputy vice-chancellor (research & innovation) at the University of Southern Queensland. His distinguished career in materials engineering and functional materials spans over 25 years, previously leading the School of Chemistry, Physics, & Mechanical Engineering at the Queensland University of Technology. A recognised authority in energy conversion, storage and nanotechnology, he has secured more than A$25 million in research funding and published in excess of 250 peer-reviewed papers. His work spans batteries, energy-efficient buildings, solar cells and carbonaceous materials. A Fellow of Engineers Australia, he champions industry-academia partnerships globally and drives real-world energy and materials innovation. Prof. Bell is also a Chief investigator on the ARC Industry Transformation Research Hub for Safe and Reliable Energy Storage (SafeREnergy).

Satyanarayanan Seshadri is associate professor in the Department of Applied Mechanics at Indian Institute of Technology Madras, India, and faculty-in-charge of its umbrella energy research initiative, the Energy Consortium. An expert in industrial energy systems, waste-heat recovery, and emissions diagnostics, he previously worked with GE Global Research and Forbes Marshall before transitioning to academia. His research group addresses energy efficiency, decarbonisation of process industries, and advanced Organic Rankine Cycle architectures. He earned a Ph.D. from Texas A&M University in aerosol science. Seshadri is recognised for translating laboratory innovations into industry-scale solutions and mentoring the next generation of clean-energy engineers.

Kothandaraman Ramanujam is a distinguished professor of electrochemistry at the Indian Institute of Technology Madras (IITM) and holds an adjunct position at the University of Southern Queensland. Prof. Ramanujam earned his Ph.D. in chemistry from the Indian Institute of Science, Bengaluru, specialising in applied electrochemistry. His research focuses on developing India-centric solutions for energy storage and conversion, such as redox flow batteries, oxide cathode and solid-state electrolyte materials for Li-ion battery, small molecule activation, such as nitrogen/nitrate/cyanide to ammonia and electrochemical reduction of carbon dioxide to syngas and formic acid. Using his innovations, he has realised large-scale (kWh to MWh) redox flow battery systems. He has received several awards for his contributions to sustainable energy materials, such as CRSI Bronze Medal, SMC Bronze Medal, ECSI Amararaja Award, IESA Researcher of the Year (2024), Masila Vijaya Award from the Academy of Chennai, and Trend Setter Grant Award from the Energy Consortium of IIT Madras.

Ashok Kumar Nanjundan, FRSC, is a professor of Energy Storage at the University of Southern Queensland, Australia, and a fellow of the Royal Society of Chemistry. England. A nanomaterials and energy expert, he formerly served as Chief Scientific Officer of a publicly listed graphene company, integrating academic research with industrial innovation. A recipient of the Marie-Curie, JSPS-Japan, and UQ Fellowships, his work focuses on carbon nanostructures and sustainable battery technologies. With over 100 publications and seven patents in journals including Chemical Reviews, ACS Nano, and Nature Protocols (h-index 55), he is globally recognised for advancing next-generation energy storage and mentoring future innovators. Prof. Nanjundan is also a chief investigator on the ARC Industry Transformation Research Hub for Safe and Reliable Energy Storage (SafeREnergy).